Article

Cell Reports

C. elegans Heterochromatin Factor SET-32 Plays an Essential Role in Transgenerational Establishment of Nuclear RNAi-Mediated Epigenetic Silencing

Graphical Abstract

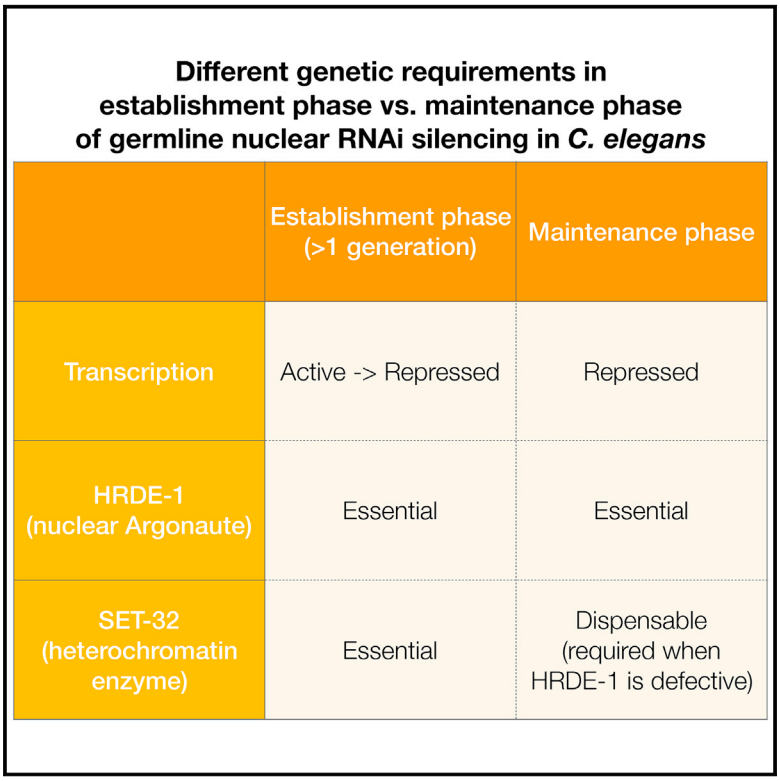

Highlights

- The onset of nuclear RNAi is a transgenerational process
- A putative histone methyltransferase, SET-32, promotes silencing establishment
- MET-2, SET-25, and SET-32 are involved for the maintenance of silencing
- For endogenous targets, their requirements are conditional on *hrde-1* mutation

Authors

Natallia Kalinava, Julie Zhouli Ni, Zoran Gajic, Matthew Kim, Helen Ushakov, Sam Guoping Gu

Correspondence

nkalinava@gmail.com (N.K.), zni@dls.rutgers.edu (J.Z.N.), zoranzg323@gmail.com (Z.G.), mmk183@scarletmail.rutgers.edu (M.K.), helen.ushakov@gmail.com (H.U.), sam.gu@rutgers.edu (S.G.G.)

In Brief

Deciphering mechanisms of transgenerational epigenetic gene regulation is critical for understanding of development, aging, and disease. In this study, Kalinava et al. examine the establishment of RNAi-mediated epigenetic silencing. The identification of the bottleneck step provides critical insight into the regulation of this pathway.

Kalinava et al., 2018, Cell Reports *25*, 2273–2284
November 20, 2018
https://doi.org/10.1016/j.celrep.2018.10.086

Cell Reports
Article

C. elegans Heterochromatin Factor SET-32 Plays an Essential Role in Transgenerational Establishment of Nuclear RNAi-Mediated Epigenetic Silencing

Natallia Kalinava,[1,*] Julie Zhouli Ni,[1,*] Zoran Gajic,[1,*] Matthew Kim,[1,*] Helen Ushakov,[1,*] and Sam Guoping Gu[1,2,*]
[1]Department of Molecular Biology and Biochemistry, Rutgers, The State University of New Jersey, Piscataway, NJ 08854, USA
[2]Lead Contact
*Correspondence: nkalinava@gmail.com (N.K.), zni@dls.rutgers.edu (J.Z.N.), zoranzg323@gmail.com (Z.G.), mmk183@scarletmail.rutgers.edu (M.K.), helen.ushakov@gmail.com (H.U.), sam.gu@rutgers.edu (S.G.G.)
https://doi.org/10.1016/j.celrep.2018.10.086

SUMMARY

The dynamic process by which nuclear RNAi engages a transcriptionally active target, before the repressive state is stably established, remains largely a mystery. Here, we found that the onset of exogenous dsRNA-induced nuclear RNAi in *C. elegans* is a transgenerational process, and it requires a putative histone methyltransferase (HMT), SET-32. By developing a CRISPR-based genetic approach, we found that silencing establishment at the endogenous targets of germline nuclear RNAi also requires SET-32. Although SET-32 and two H3K9 HMTs, MET-2 and SET-25, are dispensable for the maintenance of silencing, they do contribute to transcriptional repression in mutants that lack the germline nuclear Argonaute protein HRDE-1, suggesting a conditional role of heterochromatin in the maintenance phase. Our study indicates that (1) establishment and maintenance of siRNA-guided transcriptional repression are two distinct processes with different genetic requirements and (2) the rate-limiting step of the establishment phase is a transgenerational, chromatin-based process.

INTRODUCTION

The term RNAi originally refers to the phenomenon of exogenous dsRNA-triggered gene silencing (Fire et al., 1998; Kalinava et al., 2017; Kennerdell and Carthew, 1998), in which target mRNA is degraded by a small interfering RNA (siRNA)-associated Argonaute (AGO) protein, resulting in post-transcriptional gene silencing (PTGS) (Elbashir et al., 2001; Hammond et al., 2000, 2001; Tuschl et al., 1999). In addition to this mechanism, siRNAs can also target a gene for transcriptional gene silencing (TGS) in plants, fungi, and animals (Martienssen and Moazed, 2015; Pezic et al., 2014; Sienski et al., 2012; Wassenegger, 2000). We will use the terms classical RNAi and nuclear RNAi to refer to PTGS and TGS, respectively. Classical RNAi results in rapid degradation of exogenous dsRNA and homologous single-stranded transcripts, while long-term, stable silencing of transposons and other types of repetitive genomic elements is facilitated by nuclear RNAi.

In *C. elegans*, nuclear RNAi effects include histone modifications (H3K9me3 and H3K27me3) and transcriptional repression at endo-siRNA-targeted loci (Buckley et al., 2012; Gu et al., 2012; Guang et al., 2010; Mao et al., 2015). The study of the endogenous silencing events, which provide a rich source of targets to study the physiological functions and underlying mechanisms, is further complemented by highly manipulatable approaches using exogenous triggers such as dsRNA or transgenes (Ashe et al., 2012; Gu et al., 2012; Guang et al., 2010; Leopold et al., 2015; Minkina and Hunter, 2017; Shirayama et al., 2012). Exogenous dsRNA-induced nuclear RNAi relies on the upstream steps of classical RNAi for siRNA biogenesis (Grishok et al., 2000; Gu et al., 2012), but also requires nuclear RNAi-specific protein factors, including the germline-specific nuclear AGO protein WAGO-9/HRDE-1 (Akay et al., 2017; Ashe et al., 2012; Buckley et al., 2012; Guang et al., 2010; Shirayama et al., 2012; Spracklin et al., 2017; Weiser et al., 2017). The germline nuclear RNAi pathway is essential for various transgenerational silencing phenomena in *C. elegans* (Alcazar et al., 2008; Ashe et al., 2012; Bagijn et al., 2012; Burkhart et al., 2011; Gu et al., 2012; Leopold et al., 2015; Minkina and Hunter, 2017; Shirayama et al., 2012). In the case of exogenous dsRNA-induced heritable RNAi, the heterochromatin response, as well as the silencing effect, can persist for multiple generations after the initial dsRNA exposure (administered by feeding or injection) has been ceased (Alcazar et al., 2008; Ashe et al., 2012; Buckley et al., 2012; Grishok et al., 2000; Gu et al., 2012; Mao et al., 2015; Vastenhouw et al., 2006), providing a highly tractable system to study the transgenerational epigenetic inheritance of silencing.

The germline nuclear RNAi pathway plays an important role in maintaining genome stability (Bagijn et al., 2012; McMurchy et al., 2017; Ni et al., 2014) and is essential for germline development when *C. elegans* is under heat stress (Ashe et al., 2012; Buckley et al., 2012; Ni et al., 2016; Weiser et al., 2017). Sequencing study of HRDE-1-associated endogenous siRNAs (endo-siRNAs) suggest that a diverse set of genomic regions can be targeted by the germline nuclear RNAi pathway (Buckley et al., 2012). We previously refined the putative endogenous targets by identifying ones that lose H3K9me3, transcriptional repression, or both in mutant animals that lack HRDE-1 (Ni et al., 2014). We refer to these targets as the exemplary endogenous targets of germline nuclear RNAi, which primarily consist

of long terminal repeat (LTR) retrotransposons, but also include other types of repetitive DNA and some protein-coding genes. Interestingly, regions with germline nuclear RNAi-dependent heterochromatin (GRH) and regions with germline nuclear RNAi-dependent transcription silencing (GRTS) only partially overlap, raising the question whether the nuclear RNAi-dependent transcriptional silencing can be caused by a heterochromatin-independent mechanism (Kalinava et al., 2017; Ni et al., 2014).

To investigate the function of heterochromatin in this pathway, we and others found that germline nuclear RNAi-dependent H3K9 methylation requires multiple putative histone methyltransferases (HMTs), MET-2, SET-25, and SET-32 (Kalinava et al., 2017; Mao et al., 2015; Spracklin et al., 2017). All three proteins contain the SET domain, an evolutionarily conserved moiety that methylates the lysine residues of histone proteins. Based on the H3K9 methylation levels in the embryos of various mutant strains, MET-2 has been proposed to be a mono- and di-methylase for H3K9, and SET-25 a tri-methylase for H3K9 (Garrigues et al., 2015; Towbin et al., 2012). Mutant adults that lack SET-32 also show significant loss in the H3K9me3 chromatin immunoprecipitation (ChIP) signal (Kalinava et al., 2017). None of the three proteins have been biochemically characterized for the HMT activity. Studies using different experimental setups and target genes have reported that these putative H3K9 HMTs are required for the siRNA-guided epigenetic silencing in some cases (Ashe et al., 2012; Minkina and Hunter, 2017; Spracklin et al., 2017), but are dispensable in others (Kalinava et al., 2017; Lev et al., 2017; Minkina and Hunter, 2017). *met-2* mutant animals even exhibit the phenotype of enhanced heritable RNAi (Lev et al., 2017). We recently showed that H3K9me3 can be decoupled from transcriptional repression in nuclear RNAi (Kalinava et al., 2017). Abolishing the H3K9me3 deposition by mutating all three putative HMT genes (*met-2*, *set-25*, and *set-32*) did not lead to any de-repression at the endogenous HRDE-1 targets (the ones targeted by endo-siRNAs), nor did it cause any defects in transcriptional silencing or heritable silencing at a gene targeted by exogenous dsRNA. This argues against a simple model in which H3K9me3 plays a direct or dominant role in transcriptional repression at the nuclear RNAi targets. However, for the endogenous targets, our previous study only examined the requirement of these proteins in maintenance of silencing. It is unknown whether any of the MET-2, SET-25, and SET-32 is required for *de novo* silencing of actively transcribed endogenous targets. For studies using exogenous dsRNA-induced nuclear RNAi, worms were first exposed to dsRNA for several generations to achieve the steady-state level of repression before the silencing effects were examined (Kalinava et al., 2017). Therefore, the roles of putative H3K9 HMTs in the onset of nuclear RNAi were unknown.

In principle, a genome surveillance mechanism should consist of at least two distinct phases: establishment and maintenance of silencing. The establishment phase involves the recognition of foreign genetic material and the onset of silencing. Once initiated, the silencing state is then inherited or reinforced in the maintenance phase. In the case of exogenous dsRNA-induced nuclear RNAi, the establishment phase can be defined as the period in which dsRNA leads to the maximal level of transcriptional repression at the target gene, while the maintenance phase can be defined as the period in which a steady-state-level transcriptional repression has been reached in the presence of dsRNA. The maintenance phase is followed by the inheritance phase, in which the transcriptional repression persists, but eventually dissipates, in the progeny that are no longer exposed to dsRNA. Both the maintenance and inheritance phases of nuclear RNAi have been actively investigated. However, the establishment of the nuclear RNAi has not been carefully characterized. Previous studies observed a one-generation delay between the initial dsRNA treatment and the nuclear RNAi effects (Buckley et al., 2012; Burton et al., 2011; Gu et al., 2012), suggesting that the establishment of nuclear RNAi is a transgenerational process. It is still unknown how soon the transcriptional repression can occur after the initial dsRNA exposure. Most of the published studies rely on phenotype or protein expression to measure the silencing state. As such, a lack of transcriptional repression can be masked by an active classical RNAi (post-transcriptional silencing).

In the case of the endogenous nuclear RNAi targets (guided by endo-siRNAs), the establishment phase likely occurs soon after the first invasion of an LTR retrotransposon or other types of repetitive DNA into the *C. elegans* genome. We and others previously found that the transcription of these endogenous targets are highly active in the *hrde-1* and other nuclear RNAi mutants (Buckley et al., 2012; Ni et al., 2014, 2016), indicating that these targets still contain their transcriptional activating *cis*-regulatory elements. It remains an open question how soon a transposable element is silenced after its initial integration into the genome. Transgene has a strong tendency to be silenced in the *C. elegans* germline (Kelly et al., 1997). Interestingly, the silencing does not occur immediately after the transformation but gradually reaches the highest level over a course of multiple generations (Kelly et al., 1997), suggesting that the establishment of silencing at a transgene is a transgenerational process. The establishment process at the endogenous nuclear RNAi targets is highly important to our knowledge of genome surveillance. However, this process is largely elusive due to a lack of experimental system. Published work on the endogenous targets have been limited on the maintenance phase. In this study, we developed different strategies to examine the establishment process of silencing for an exogenous dsRNA target and endogenous targets. In these experiments, both types of targets started with active transcription. We monitored the onset of repression for multiple generations, and, for the endogenous targets, at the whole-genome level. We found that the establishment of nuclear RNAi is a transgenerational process and requires SET-32 and SET-25, although at different degrees.

RESULTS

The Onset of Nuclear RNAi-Mediated Silencing in Wild-Type Animals Occurs One Generation after the Exogenous dsRNA Exposure

To investigate the transgenerational onset of nuclear RNAi, we performed a five-generation *oma-1* RNAi experiment by feeding worms with *oma-1* dsRNA-expressing *E. coli* (Figure 1A). *oma-1* is a non-essential germline-specific gene (Lin, 2003) and has

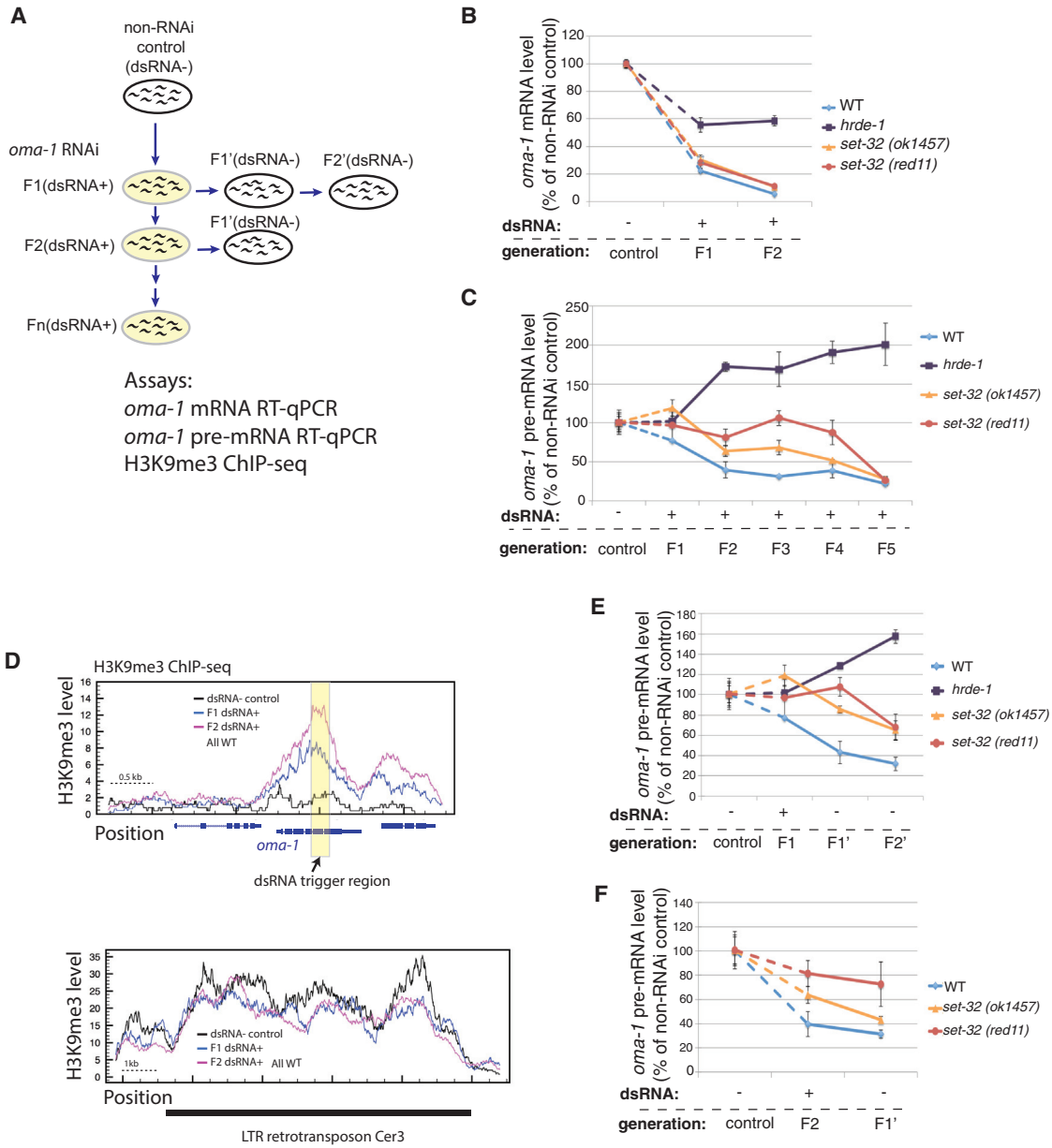

Figure 1. Multigenerational Analysis of Exogenous dsRNA-Triggered RNAi at *oma-1*

(A) A schematic of the experiment. F1–F5(dsRNA$^+$), adult animals fed on *oma-1* dsRNA-expressing *E. coli* for one to five generations, were used to test the establishment of silencing. F1′ and F2′(dsRNA$^-$), the first and second generation after shifting from *oma-1* dsRNA$^+$ to dsRNA$^-$, were used to test the inheritance of silencing.

(B) *oma-1* mRNA RT-qPCR analysis of the control (dsRNA$^-$), F1(dsRNA$^+$), and F2(dsRNA$^+$) samples.

(C) *oma-1* pre-mRNA RT-qPCR analysis of the control (dsRNA$^-$) and F1–F5(dsRNA$^+$) samples. This is one of two biological replicates for this experiment. The second one is shown in Figure S1.

(D) H3K9me3 ChIP-seq coverage plots for the *oma-1* locus (top panel) and LTR retrotransposon Cer3 (bottom panel). Wild-type animals of control (dsRNA$^-$), F1(dsRNA$^+$), and F2(dsRNA$^+$) were used. Cer3, used as a control locus here, is an endogenous HRDE-1 target with a high level of H3K9me3, which is not affected by *oma-1* RNAi. All profiles are normalized by total reads aligned to the whole genome.

(E) *oma-1* pre-mRNA RT-qPCR analysis of the progeny (F1′[dsRNA$^-$] and F2′[dsRNA$^-$]) of the F1(dsRNA$^+$) animals.

(F) *oma-1* pre-mRNA RT-qPCR analysis of the progeny (F1′[dsRNA$^-$]) of the F2(dsRNA$^+$) animals. The values for the control, F1(dsRNA$^+$), and F2(dsRNA$^+$) samples from (C) are also used in (E) and (F) for comparison. Each RT-qPCR result in (B), (C), (E), and (F) represent the mean value of n = 3; whiskers represent the SD.

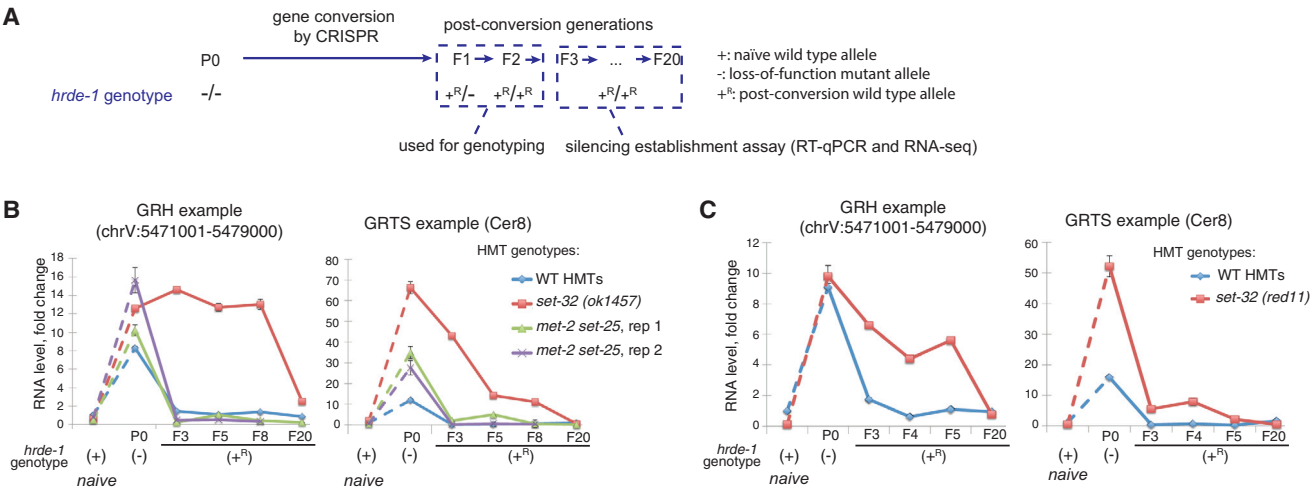

Figure 2. Silencing Establishment Assay of Endogenous HRDE-1 Targets

(A) A schematic of the silencing establishment assay using CRISPR-Cas9-mediated gene conversion of the *hrde-1(tm1200)* mutation to the wild-type sequence. (B and C) RT-qPCR analysis for two endogenous HRDE-1 targets at pre- and post-conversion generations, as well as samples with the identical genotypes as the post-conversion generations but without experiencing the *hrde-1* mutation (naive samples). RNA expressions in different samples were normalized to the ones in the wild-type strain (N2). Two biological replicates were shown in (B) and (C). Each RT-qPCR value in (B) and (C) represents the mean value of n = 3; whiskers represent the SD. The GRH locus used in this analysis is chrV:5471001–5479000. The GRTS locus used in this analysis is LTR retrotransposon Cer8, located at chrV:5179680–5191222. (GRH, germline nuclear RNAi-mediated heterochromatin; GRTS, germline nuclear RNAi-mediated transcriptional silencing. GRH and GRTS regions, as well as the annotated genes located in these regions, were from Tables S1–S3 of Ni et al., 2014).

been routinely used to study nuclear RNAi and epigenetic inheritance of silencing. In this experiment, young adult worms that were exposed to *oma-1* dsRNA for one to five generations were collected (referred to as F1[dsRNA$^+$] to F5[dsRNA$^+$] animals). Adult worms fed on *E. coli* OP50, which does not express any worm-specific dsRNA, were used as the control (dsRNA$^-$ control).

To examine the nuclear RNAi-mediated silencing at *oma-1*, we measured the *oma-1* pre-mRNA levels by using RT-qPCR, with random hexamer oligoes as the RT primer and an *oma-1* intron-specific and an exon-specific primer for the qPCR. To examine the combined effects of classical RNAi and nuclear RNAi at *oma-1*, we measured the *oma-1* mature mRNA levels using the oligo-dT as the RT primer and two exon-specific primers for the qPCR. The same strategy has been used in our previous study (Kalinava et al., 2017).

The wild-type animals exhibited robust repression of *oma-1* at the mRNA level in F1(dsRNA$^+$), with approximately 78% reduction compared to the dsRNA$^-$ control animals (Figure 1B). Further reduction in *oma-1* mRNA was observed in the F2(dsRNA$^+$) animals.

Compared to the repression measured at the *oma-1* mRNA level, the one at the pre-mRNA level was delayed by one generation in wild-type animals. The level of *oma-1* pre-mRNA was reduced by 23% or remained unchanged in F1(dsRNA$^+$) animals compared to the dsRNA$^-$ control (two biological replicates; Figures 2C and S1). The levels of *oma-1* pre-mRNAs in F2–F5(dsRNA$^+$) samples were relative stable, at approximately 40% of the one in the dsRNA$^-$ control. This result suggests a difference in the speed of onset between classical RNAi and nuclear RNAi in wild-type animals: a robust silencing mediated by the classical RNAi begins within the first generation of dsRNA exposure, and a robust silencing mediated by the nuclear RNAi begins at the second generation.

We also examined the level of H3K9me3 at the *oma-1* locus in the same samples of the F1(dsRNA$^+$) and F2(dsRNA$^+$) wild-type animals by performing H3K9me3 chromatin immunoprecipitation sequencing (ChIP-seq) analysis. We found that both samples exhibited high levels of H3K9me3 in *oma-1* gene (Figure 1D), and the levels were similar to our previously reported level in animals treated with *oma-1* dsRNA for three to four generations (Kalinava et al., 2017). Therefore, the onset of robust H3K9me3 at *oma-1* begins at the first generation of dsRNA exposure, one generation earlier than the transcriptional repression.

As a control for the requirement of nuclear RNAi for the observed transcriptional repression of *oma-1,* we examined the *oma-1* pre-mRNA and mRNA levels in *hrde-1* mutant animals fed with *oma-1* dsRNA. Similar to N2, *oma-1* expression at the pre-mRNA level was not repressed in the F1(dsRNA$^+$) *hrde-1* animals (Figure 1C), confirming the requirement of nuclear RNAi for the transcriptional repression. Interestingly, *oma-1* RNAi led to a progressive increase in *oma-1* pre-mRNA level in the F2–F5(dsRNA$^+$) *hrde-1* animals. The same effect was observed in our previous study (Kalinava et al., 2017). Here, we also performed the *oma-1* RNAi experiment in *nrde-2* mutant strain for three generations, which is also defective in nuclear RNAi (Guang et al., 2010), and again observed progressively increased *oma-1* pre-mRNA levels compared to dsRNA$^-$ control *nrde-2* mutant animals (Figure S1A). These results suggest that exogenous dsRNA can affect transcription or co-transcriptional RNA processing in a nuclear RNAi-independent manner. Future studies are required to investigate the nature of such effect.

Despite the increased pre-mRNA, we observed approximately 40% reduction in *oma-1* mRNA in both the F1(dsRNA$^+$) and F2(dsRNA$^+$) *hrde-1* animals compared to the dsRNA$^-$ control *hrde-1* animals (Figure 1B). The reduction is consistent with the previous finding that the classical RNAi is active in the *hrde-1* mutant (Buckley et al., 2012; Kalinava et al., 2017). However, the *oma-1* mRNA levels in the F1(dsRNA$^+$) and F2(dsRNA$^+$) *hrde-1* animals were much higher than the F1(dsRNA$^+$) and F2(dsRNA$^+$) wild-type animals (Figure 1B). This may due to the active transcription of *oma-1*, a partial defect of classical RNAi in the *hrde-1* mutant, or both. Further study is required to distinguish these possibilities.

set-32 Mutation Results in a More Gradual, Multigenerational Establishment of exo-dsRNA-Induced Transcriptional Repression

To investigate whether any of the putative H3K9 HMTs plays a role in the establishment of transcriptional repression, we performed multigenerational *oma-1* RNAi experiments using *set-32*, *met-2*, and *set-25* single-mutant strains, as well as the *met-2 set-25* double mutant. Two different *set-32* mutant alleles were used in this study. One is the *set-32(ok1457)* allele (C. elegans Deletion Mutant Consortium, 2012) which has an in-frame deletion of 156 aa (position 50–205), located before the SET domain, and has been used in previous studies (Ashe et al., 2012; Kalinava et al., 2017). In this study, we also used clustered regularly interspaced short palindromic repeats (CRISPR) to generate a second allele, *set-32(red11)*, which lacks the SET domain. We measured the dsRNA-induced H3K9me3 at *oma-1* using this new allele (three to four generations of dsRNA$^+$), and found that, same as *set-32(ok1457)*, *set-32(red11)* caused a significant reduction in, but did not completely abolish, the RNAi-induced H3K9me3 (Figure S2C). Also, the same as previously observed for the *set-32*(*ok1475*) mutant (Kalinava et al., 2017), *set-32*(*red11*) mutant animals exhibited no defect in heritable RNAi after three to four generations of exo-dsRNA exposure (Figures S2A and S2B). For the onset of silencing, *oma-1* mRNA was robustly silenced by RNAi in both *set-32* mutant alleles at the first generation of the dsRNA exposure, similar to wild-type animals (Figure 1B). Interestingly, the onset of nuclear RNAi, measured by pre-mRNA, was much slower in *set-32* mutant than the wild-type animals. Both *set-32* mutant alleles generally had higher *oma-1* pre-mRNA than wild-type animals in the first four dsRNA$^+$ generations (Figures 1C and S1). It was at the fifth generation when the repression reached the steady-state level observed in the wild-type animals (Figures 1C and S1). Therefore, *set-32* mutation causes a multigenerational delay in dsRNA-triggered transcriptional repression. We also tested *met-2*, *set-25*, and *met-2 set-25* mutant animals. All three mutants exhibited wild-type-like profiles in pre-mRNA repression at the first and second generations of the dsRNA exposure (Figure S1B). These results suggest that, although both SET-32 and MET-2 SET-25 contribute to the H3K9me3 at the RNAi target, their functions are not equivalent. SET-32-dependent activity, but not MET-2 SET-25-dependent activity, promotes the onset of exogenous dsRNA-induced transcriptional repression. The SET domain of SET-26 can methylate H3K9 *in vitro* (Greer et al., 2014). We previously showed that neither SET-26 nor SET-9, which is 96% identical to SET-26 at the amino acid level, is required for the dsRNA-induced H3K9me3 at *oma-1* (Kalinava et al., 2017). Here, we found that the *set-9 set-26* double mutant had no defect in the onset of the dsRNA-induced transcriptional repression at *oma-1* (Figures S1C and S1D).

To examine inheritance of silencing induced by a shorter duration of dsRNA exposure (one or two generations as opposed to four), we cultured the progeny of dsRNA-exposed animals on OP50 plates that lacked *oma-1* dsRNA for one or two generations (referred to as inheritance generations) (Figure 1A). For wild-type animals, both one-generation and two-generation dsRNA exposures resulted in robust repression at the pre-mRNA level in the inheritance generations (Figures 1E and 1F). Interestingly, after only one generation of dsRNA exposure, the first and second inheritance generations showed progressively stronger *oma-1* repression at the pre-mRNA levels (Figure 1E), suggesting that the transgenerational establishment of transcriptional repression does not require continuous dsRNA exposure. For *set-32* mutants, we again observed delayed nuclear RNAi in the inheritance generations (Figures 1E and 1F), confirming the role of SET-32 in promoting the establishment of nuclear RNAi-mediated silencing.

Developing a CRISPR-Based Approach to Study the Establishment of Silencing at the Endogenous Targets of Germline Nuclear RNAi

One challenge of studying the establishment of silencing at the endogenous targets (ones targeted by endo-siRNAs) is to begin with an actively transcribed target for the experiment. This can be achieved at the whole-genome level by using a nuclear RNAi-defective mutant, such as *hrde-1*, in which a defined set of endogenous targets are actively transcribed (Buckley et al., 2012; Ni et al., 2014, 2016). To examine the establishment of silencing at these endogenous targets, we used CRISPR-mediated gene conversion to repair the loss-of-function *hrde-1*(*tm1200*) mutation in worms that had carried the *hrde-1* mutation for more than 20 generations. We wanted to know how fast the repressive states can be established at the endogenous nuclear RNAi targets when the HRDE-1 activity is restored. Besides the CRISPR method, a wild-type *hrde-1* allele can also be introduced to the *hrde-1* mutant strain via a genetic cross. We did not choose this method because genetic crosses will introduce epigenetically repressed alleles of the endogenous targets, as well as a foreign siRNA population.

To repair the *hrde-1* mutation using CRISPR, a mixture of *hrde-1*-targeting Cas9 ribonuclease complex and repair template DNA was injected into the gonads of *hrde-1* mutant hermaphrodite adults (Figure 2A). The wild-type *hrde-1* allele generated by gene conversion was annotated as *hrde-1*(+^{R}), and the naive wild-type *hrde-1* allele (i.e., an allele that never experienced any mutation) as *hrde-1*(+). Progeny of the injected animals were produced by self-fertilization throughout the experiment. The F1 *hrde-1*(+^{R}/–) and F2 *hrde-1*(+^{R}/+^{R}) individuals were identified by PCR and Sanger sequencing. We then collected later generations of the homozygous *hrde-1*(+^{R}) adults and examined the abundance of the transcripts of the endogenous targets. The F3 was the earliest generation that can be collected for the assay because the F1 and F2 progeny were

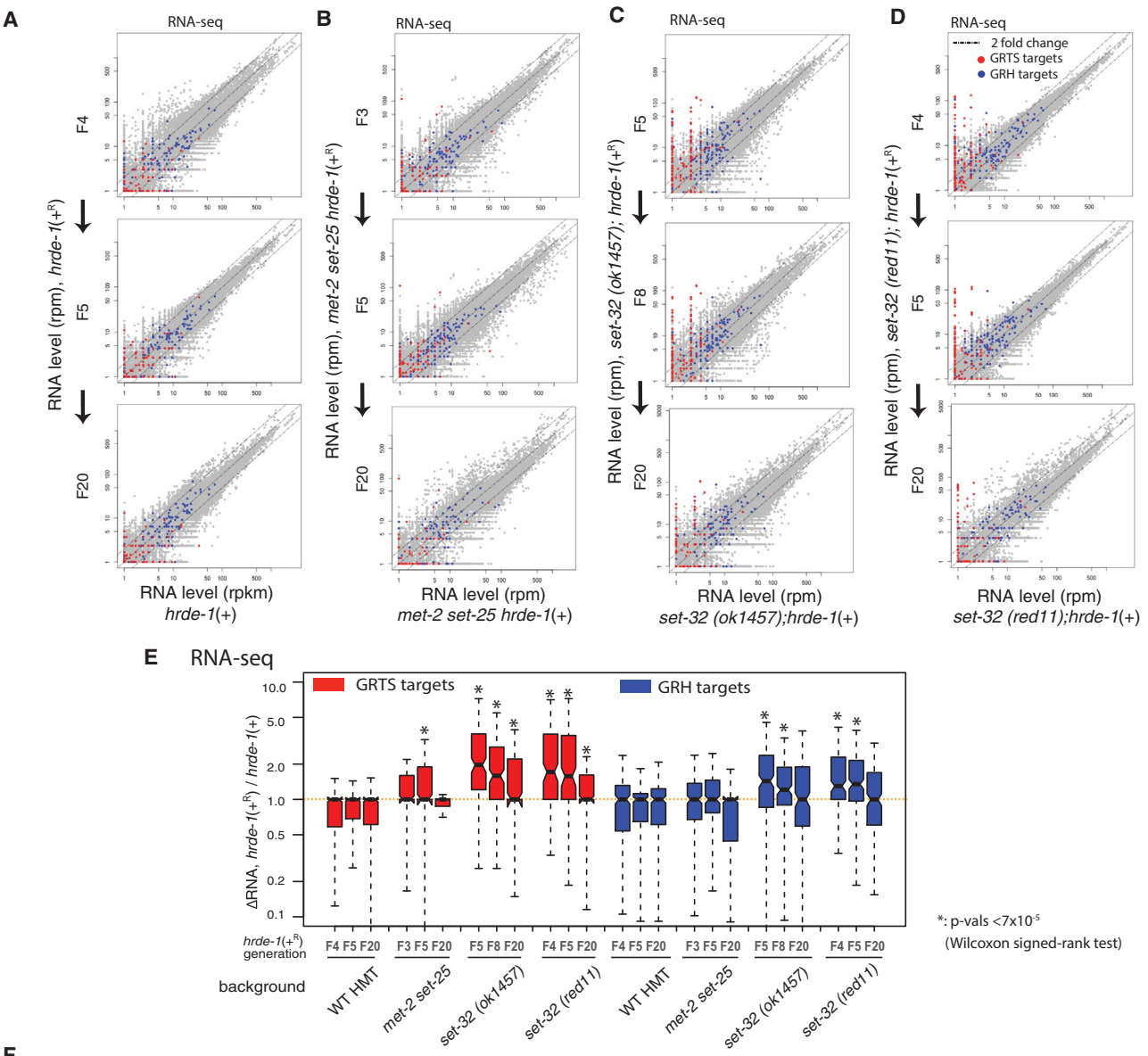

(legend on next page)

used for genotyping. We measured the abundance of the transcripts for two endogenous targets by RT-qPCR. Both established their repressive states in the F3 *hrde-1*(+^{R}) and later generations (two biological replicates; Figures 2B and 2C). We also identified the F2 *hrde-1*(−/−) individuals and collected their progeny (F3) and performed RT-qPCR analysis (Figure S3D). The endogenous targets remained de-repressed in the F3 *hrde-1*(−/−) progeny (Figure S3D), as expected. These results indicate that silencing of endogenous targets can be established at the F3 generation after repairing the *hrde-1* mutation by gene conversion.

SET-32 Is Required for the Establishment of Silencing for Some of the Endogenous Targets

To test whether the putative H3K9 HMTs are required for establishment of silencing at the endogenous targets, we generated *set-32;hrde-1* and *met-2 set-25 hrde-1* mutant strains. Two different alleles (*ok1457* and *red11*) of *set-32* mutations were used this experiment. For *set-32(ok1457)*, we collected F3, F5, F8, and F20 populations after the gene conversion. For *set-32(red11)*, we collected F3, F4, F5, and F20 populations. Both *set-32* alleles exhibited a delay in the establishment of silencing for eight or five generations. Full repressions of these targets were reached at the F20 generation (Figures 2B and 2C). We confirmed that the early generations of the *hrde-1*(+^{R}) animals had similar *hrde-1* mRNA expressions as the *hrde-1*(+) animals (Figure S3). Therefore, the delayed establishment of silencing is not due to a lower *hrde-1* mRNA expression in the early post-conversion generations. For the *met-2 set-25 hrde-1* mutant strain, two independent lines of *met-2 set-25 hrde-1* [+^{R}/+^{R}] worms were followed and both fully established the repressive states by the F3 generation for the two tested targets (Figure 2B).

To examine the establishment of silencing at the whole-genome level, we performed RNA sequencing (RNA-seq) for the post-conversion populations (*hrde-1*[+^{R}/+^{R}], *set-32;hrde-1* [+^{R}/+^{R}], and *met-2 set-25 hrde-1*[+^{R} /+^{R}]), as well as animals of the identical genotypes but with the naive wild-type *hrde-1* allele (*hrde-1*[+/+], *set-32;hrde-1*[+/+], and *met-2 set-25 hrde-1*[+/+]). We sequenced rRNA-depleted total RNA of each sample in order to include both polyadenylated RNA and non-polyadenylated RNA. For the post-conversion samples, we performed RNA-seq for the F4, F5, and F20 populations for *hrde-1*(+^{R}), F3, F5, and F20 for *met-2 set-25 hrde-1*(+^{R}), F5, F8, and F20 for *set-32(ok1457) hrde-1*(+^{R}), and F4, F5, and F20 for *set-32(red11) hrde-1*(+^{R}). Our whole-genome analysis indicated that repairing *hrde-1* mutation fully silenced all of the endogenous targets as early as in the F4 post-conversion population of the animals carrying the wild *type met-2*, *set-25*, and *set-32* genes (Figures 3A and 3E). In contrast, some of the endogenous targets remained actively expressed even in the F20 post-conversion populations of animals carrying either the *set-32(red11)* or *set-32(ok1457)* mutation (Figures 3C–3E). These targets are referred to as putative irreversible targets. After examining the RNA-seq profiles individually, we identified four exemplary irreversible targets, which include two LTR retrotransposons (Cer9 and Cer12), a putative protein-coding gene *c38d9.2* in chromosome V, and an approximately 5-kb region in chromosome II (containing two uncharacterized putative protein-coding genes *f15d4.5* and *f15d4.6*) (Figures 3F and S5–S8). All of these loci became transcriptional activated in *hrde-1* and *set-32;hrde-1* mutants, but remained silent in *set-32* mutant (with naive wild-type *hrde-1*), despite the losses of H3K9me3 at these regions (Figures 3F and S5–S8). These data confirm our previous finding that SET-32 is dispensable for the maintenance of silencing at the native HRDE-1 targets (Kalinava et al., 2017). These irreversible targets represent a bona fide epigenetic phenomenon in which two genetically identical populations (cultured in the same conditions and harvested at the same developmental stage) exhibit different gene expression profiles.

We found that *met-2 set-25* are required for the establishment of silencing in only one of the four irreversible targets, *c38d9.2* (Figure S7). Our global analysis indicated that most of the endogenous targets established the silencing states as early as in the F3 *met-2 set-25 hrde-1*(+^{R}) populations (Figures 3B and 3E).

We also performed the silencing establishment assay using the *set-32;met-2 set-25 hrde-1* mutant strain. All four irreversible targets identified in the *set-32* mutant ground failed to initiate the silencing the F5 *set-32;met-2 set-25 hrde-1*(+^{R}) population (Figures S4–S8). The expression levels of these targets in F5 *set-32;met-2 set-25 hrde-1*(+^{R}) and F5 *set-32; hrde-1*(+^{R}) were similar.

We note that majority of the irreversible targets in *set-32* mutant belong to the GRTS regions. In contrast, most of the GRH regions restored the transcriptional repression by the F4–F5 post-repair generation in the *set-32* mutant background (Figures 3C–3E). Taken together, our results indicate that SET-32 is required for the establishment of the repression states of some endogenous HRDE-1 targets. Although *met-2 set-25* mutant animals had a much weaker phenotype than *set-32* in this assay, we cannot rule out that MET-2 and SET-25 are required for the establishment of silencing in the first and second post-conversion generations, which were precluded in the assay due to the screening procedure after CRISPR.

Figure 3. RNA-Seq Analysis of Silencing Establishment at Endogenous HRDE-1 Targets

(A–D) Scatterplot analysis of normalized RNA-seq counts for all 1-kb genomic regions comparing animals in the post-conversion generations with animals of the same genotype but without experiencing *hrde-1* mutation (naive samples). (A) Wild-type *set-32;met-2 set-25* background, (B) *met-2 set-25* double-mutant background, (C) *set-32(ok1457)* background, and (D) *set-32(red11)* background. GRTS and GRH regions (see Figure 1 legend for their definitions) are colored in red and blue, respectively.

(E) Boxplot analysis of the changes in RNA expression of GRTS or GRH regions between post-conversion animals and the corresponding naive samples.

(F) An exemplary endogenous HRDE-1 target (LTR retrotransposon Cer9) that is defective in silencing establishment in the *set-32* mutant for at least 20 generations, but not in the *met-2 set-25* mutant. Normalized total RNA-seq signals were plotted. Columns from left to right are the naive samples (*hrde-1[+]*), pre-conversion samples (*hrde-1[-]*), and F5 and F20 post-conversion samples (*hrde-1[+^{R}]*). Different genetic backgrounds (wild-type [WT] or various H3K9 HMT mutants) are in different rows as indicated. All results represented here are normalized by total reads aligned to the whole genome.

*$p < 7 \times 10^{-5}$ (Wilcoxon singed-rank test).

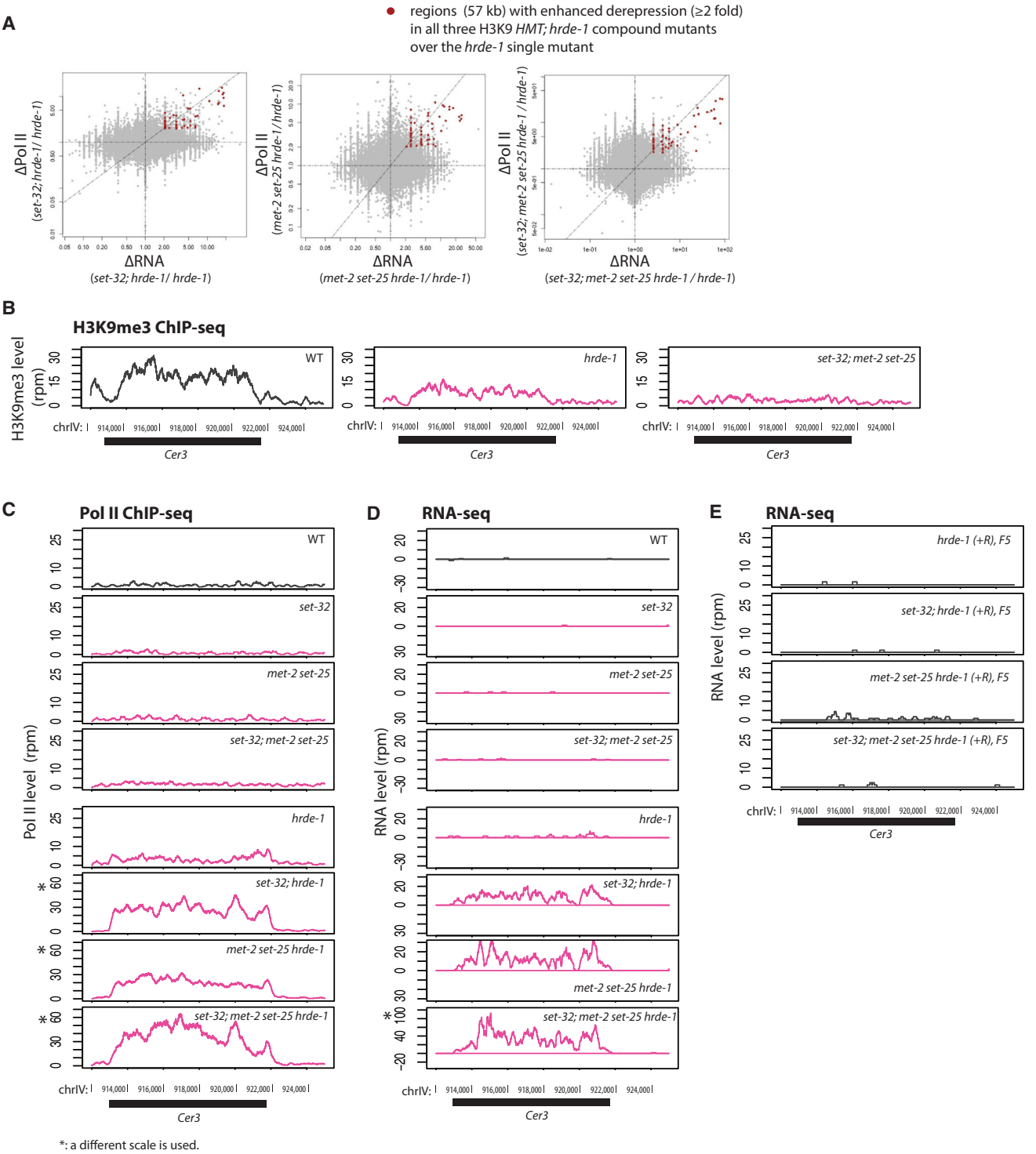

Figure 4. Enhanced Silencing Defects in the Endogenous HRDE-1 Targets Caused by the Combination of H3K9 HMT and *hrde-1* Mutations

(A) Scatterplots with changes in RNA-seq signals between a compound mutant and *hrde-1* single mutant plotted in the x axis and changes in Pol II ChIP-seq signals plotted in the y axis for all 1-kb genomic regions. Regions with ≥2-fold increases in both RNA expression and Pol II occupancy in all three *H3K9 hmt;hrde-1* compound mutants over *hrde-1* single mutant were marked with red dots.

(legend continued on next page)

To explore the role of endo-siRNAs in the establishment of silencing, we performed small RNA-sequencing (sRNA-seq) analysis for the pre-conversion samples, the F5 and F20 post-conversion generations, and the matching samples with the naive wild-type *hrde-1* allele. We found that the endo-siRNA profiles at the irreversible targets in *set-32 hrde-1*(+) was similar to the ones in the wild-type (WT) animals, arguing against an active role of SET-32 in promoting the endo-siRNA levels at these targets. The *set-32 hrde-1*(−) and the post-conversion *set-32 hrde-1*($+^{R}$) animals had abundant endo-siRNAs at the irreversible targets. Their profiles were different from the ones in the *set-32 hrde-1*(+) but similar to the ones in the *hrde-1*(−) animals (Figures S5–S8). These results argue against the possibility that the delayed establishment of silencing observed in *set-32* mutant is caused by a lag in endo-siRNA expression. The changes in the endo-siRNA expressions in the *set-32 hrde-1*(−) and the post-conversion *set-32 hrde-1*($+^{R}$) animals, in comparison to WT animals, are likely due to the increased transcripts of the irreversible targets, which template the endo-siRNA synthesis.

H3K9 HMTs Are Required to Maintain the Repressive States for Some Endogenous HRDE-1 Targets in *hrde-1* Mutant Animals

We performed Pol II ChIP-seq and RNA-seq analyses for various compound mutants including *set-32;hrde-1*, *met-2 set-25 hrde-1*, and *set-32;met-2 set-25 hrde-1*. As expected, the endogenous HRDE-1 targets were de-repressed in these compound mutants (Figures S9A and S9B). Intriguingly, for a small subset of the targets, the *hmt; hrde-1* compound mutants exhibited much higher RNA expression and Pol II occupancy than the *hrde-1* single mutant (Figures 4A and S5), indicating that the loss of H3K9me3 further enhances the *hrde-1* mutation's defects in transcriptional repression for these targets. Such enhancement is unexpected because *set-32*, *met-2 set-25*, *set-32;met-2 set-25* mutant animals have no silencing defects at the endogenous targets, as reported previously (Kalinava et al., 2017) and shown again using the new data generated in this study (Figure S9). An exemplary endogenous target with such enhanced de-repression is the LTR retrotransposon Cer3 (Figures 4B–4D). Either *set-32* single or *met-2 set-25* double mutations, when combined with the *hrde-1* mutation, drastically increased the Pol II occupancy at Cer3 and Cer3 transcripts. Therefore, the enhanced de-repression occurs at the transcriptional level. The enhanced de-repression caused by different H3K9 HMTs appears to be additive because the quadruple mutant of *set-32;met-2 set-25 hrde-1* showed the highest Cer3 expression (Figures 4C and 4D). Interestingly, Cer3 is not an irreversible target (Figure 4E). These results indicate that, for a small subset of the endogenous targets, H3K9me3 HMTs are required for the maintenance of repression. However, such requirements are only apparent when HRDE-1 activity is compromised. We note that, for the majority of the endogenous HRDE-1 targets, the combined mutations in *H3K9* HMT genes and *hrde-1* had no additive effect of de-repression compared to the *hrde-1* single mutant (Figure S9).

DISCUSSION

The Establishment and Maintenance Phases of Germline Nuclear RNAi in *C. elegans*

H3K9me3 is an evolutionarily conserved nuclear RNAi effect in fungi, plants, and animals. In *C. elegans*, this effect is highly specific and prominent at target loci. Furthermore, it is transgenerationally heritable and linked to the germline immortality (Ashe et al., 2012; Buckley et al., 2012; Burton et al., 2011; Gu et al., 2012; Shirayama et al., 2012; Weiser et al., 2017). H3K9me3 at nuclear RNAi targets requires three putative HMTs: MET-2, SET-25, and SET-32 (Kalinava et al., 2017; Mao et al., 2015; Spracklin et al., 2017). Strikingly, we previously found that a complete loss of H3K9me3 in the mutant worms that lack the three HMTs did not cause any defect in transcriptional repression at the endogenous targets (Kalinava et al., 2017). The experimental setup in the previous study was designed to examine the maintenance of silencing and precluded us from studying the establishment phase. For a newly inserted transposon that is transcriptionally active, the establishment phase precedes the maintenance phase and two phases may involve different mechanisms.

Exo-dsRNA-triggered nuclear RNAi provides an inducible system in which to study the establishment, maintenance, and inheritance of epigenetic silencing at a gene that is normally actively expressed. The previous discovery of a transgenerational delay in the onset of H3K9me3 at the target gene (Burton et al., 2011; Gu et al., 2012) suggests that the establishment of nuclear RNAi is a gradual process. The kinetics of transcriptional repression during the early generations of dsRNA exposure have not been examined before this study.

In this study, we examined the establishment phase for both endo-siRNA-guided and exogenous dsRNA-triggered nuclear RNAi. Based on the results of this and our previous work (Kalinava et al., 2017), we propose a model in which the establishment and maintenance phases of nuclear RNAi have the following distinctions (Figure 5).

(1) The transcriptional state of the target locus. At the maintenance phase, the target is stably repressed and kept in a heterochromatic state. In contrast, the establishment phase begins with an actively transcribed and euchromatic state at the target locus. Converting from an active state to a stably repressed state requires removal of euchromatic marks and the deposition of heterochromatic marks. Therefore, the speed of the silencing establishment may depend on the relative strengths of the two opposing forces.

(B–D) The H3K9me3 ChIP-seq (data from Kalinava et al., 2017) (B), Pol II ChIP-seq (S2 phosphorylated) (C), and RNA-seq (D) coverage plots at the LTR retrotransposon Cer3 in WT and various mutant animals. Panels marked with an asterisk (*) use a different scale to accommodate the enhanced expression levels observed for the genotype.

(E) RNA-seq profiles at Cer3 for post-conversion samples (*hrde-1*[$+^{R}/+^{R}$]) with WT H3K9 HMT genes or various H3K9 HMT mutations. All results represented in this figure are normalized by total reads aligned to the whole genome.

A

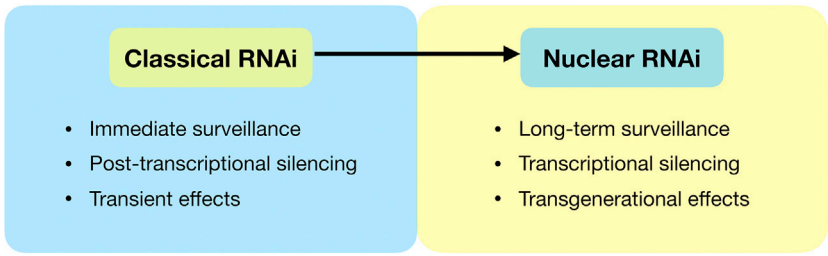

B

Different genetic requirements in establishment phase vs. maintenance phase of gremline nuclear RNAi silencing in *C. elegans*

	Establishment phase (>1 generation)	Maintenance phase
Transcription	Active -> Repressed	Repressed
HRDE-1 (nuclear Argonaute)	Essential	Essential
SET-32 (heterochromatin enzyme)	Essential	Dispensable (required when HRDE-1 is defective)

Figure 5. Functional and Mechanistic Differences between Classical RNAi and Nuclear RNAi, and Different Phases of Nuclear RNAi in *C. elegans*

(A) Classical RNAi provides an immediate silencing response at the same generation when animals are exposed to dsRNA. Classical RNAi silencing is at the post-transcriptional level, and is not transgenerationally heritable. In contrast, nuclear RNAi silencing takes more than one generation to be established. Nuclear RNAi represses target loci at the transcriptional level and is heritable. It provides long-term transgenerational silencing.

(B) Establishment and maintenance phases of nuclear RNAi involve different transcriptional activities and genetic requirements.

(2) Silencing mechanism. We propose that nuclear RNAi consists of multiple distinct silencing mechanisms. One of these mechanisms is an H3K9me3-independent silencing mechanism, which likely is the main source of silencing during the maintenance phase. The active transcription during the establishment phase may pose a strong force against the H3K9me3-independent silencing mechanism. Such antagonistic interactions between euchromatin (H3K36me3) and heterochromatin have been shown to occur in the *C. elegans* germline (Gaydos et al., 2012; Weiser et al., 2017). It is conceivable that SET-32-dependent H3K9me3 promotes the onset of silencing, either by providing an additional force of repression (H3K9me3-dependent in this case) or by enhancing the efficacy of H3K9me3-independent silencing mechanism. However, given enough time, H3K9me3-independent mechanisms can eventually establish silencing in the absence of SET-32. Although the prolonged lag in silencing is tolerated by the mutant worms at the organismal level in the laboratory condition, this molecular defect may create a window for the transposition of a newly invaded mobile DNA, and therefore it is likely to be selected against in a wild population.

The establishment phase of an epigenetic silencing phenomenon is often difficult to study because of its transient nature. The *set-32* mutation slows down the onset of silencing and therefore provides an expanded window to dissect the extraordinarily complex process.

Although MET-2, SET-25, and SET-32 all contribute to the H3K9me3 at the nuclear RNAi targets, SET-32 and MET-2 SET-25 are not equivalent in their role in silencing establishment. This may due to differential expression of these proteins. Alternatively, the functional difference could be due to certain unknown H3K9me3-independent activities associated with individual enzymes. Future study is required to investigate these possibilities. In agreement with our finding, the study by Woodhouse et al. (2018) (in this issue of *Cell Reports*) found that SET-32 is required for the establishment of transgenerational silencing induced by dsRNA at a gfp reporter gene. The Ashe group found that SET-25 is also required in the establishment. We found that SET-25 is required for the silencing establishment for one of the endogenous targets, but not the other SET-32-dependent ones, including the exogenous dsRNA-targeted *oma-1*. This difference is perhaps due to different chromatin structures and transcription activities at the target genes.

What Is the Functional Significance of the One-Generation Delay in Exo-dsRNA-Induced Nuclear RNAi?

Although exo-dsRNA was used as an artificial means to induce RNAi in this study, it is akin to a situation in which host animals encounter viral nucleic acids. We speculate that such a delay is a consequence of the specialization of classical RNAi and nuclear RNAi: the former eliminates the immediate threat by degrading the target RNA, and the latter provides long-term silencing at the chromatin level, which is critical for the control of retroviruses or retrotransposons. One possible benefit of the delay of nuclear RNAi is to allow the biogenesis of secondary siRNAs (Pak and Fire, 2007; Sijen et al., 2007), which requires mRNA as template for the RdRP activity. If both nuclear RNAi and classical RNAi are fully active at the initial encounter of dsRNA, germ cells may not be able to produce sufficient siRNAs to facilitate silencing inheritance.

CRISPR Provides a Unique Advantage for Studying Transgenerational Epigenetics

In this study, we used CRISPR-mediated gene editing to repair a mutation in the *hrde-1* gene, which allowed us to capture the

graduate changes in the endogenous targets after the nuclear RNAi machinery is turned on in the subsequent generations. This approach is analogous to heat or small molecule-inducible gene expression, but without the need to change the native promoter or protein sequence of the inducible gene. This approach also avoids crossing two strains carrying different genetic and epigenetic backgrounds, which makes this approach highly tractable. (For example, there is no need to distinguish different epialleles.)

Our study showed that, after repairing *hrde-1*, WT animals fully restored silencing at the endogenous targets in the third generation. Our current implementation of CRISPR does not allow us to examine the first and second generations after the HRDE-1 activity is restored. The one-generation delay observed for the exo-dsRNA-triggered nuclear RNAi raises a possibility that the establishment of silencing at the endogenous targets may also have a transgenerational delay even in a WT H3K9 HMT background.

CRISPR-mediated genome editing provides a powerful tool for biomedical research and curing genetic diseases. Our study provides a cautionary example that repairing a mutated gene may not immediately restore the normal function expected for the WT allele. Therefore, epigenetic effects must be considered when editing genes, especially when chromatin factors and epigenetic pathways are involved.

STAR★METHODS

Detailed methods are provided in the online version of this paper and include the following:

- KEY RESOURCES TABLE
- CONTACT FOR REAGENT AND RESOURCE SHARING
- EXPERIMENTAL MODEL AND SUBJECT DETAILS
- METHOD DETAILS
  - oma-1 RNAi experiments
  - Gene conversion to repair hrde-1 mutation using CRISPR-Cas9
  - Total RNA extraction
  - mRNA and pre-mRNA RT-qPCR
  - High-throughput sequencing
- QUANTIFICATION AND STATISTICAL ANALYSIS
- DATA AND SOFTWARE AVAILABILITY

SUPPLEMENTAL INFORMATION

Supplemental Information includes nine figures and two tables and can be found with this article online at https://doi.org/10.1016/j.celrep.2018.10.086.

ACKNOWLEDGMENTS

We thank Elaine Gavin, Shobhna Patel, Monica Driscoll, Lamia Wahba, and Andy Fire for help and suggestions. Research reported in this publication was supported by the Busch Biomedical Grant and the National Institute of General Medical Sciences of the NIH, United States, under Award R01GM111752. Some strains were provided by the CGC, United States, which is funded by NIH Office of Research Infrastructure Programs (P40 OD010440). The content is solely the responsibility of the authors and does not necessarily represent the official views of the NIH.

AUTHOR CONTRIBUTIONS

Conceptualization, N.K. and S.G.G.; Methodology, N.K., J.Z.N., and S.G.G.; Investigation, N.K., J.Z.N., Z.G., M.K., and H.U.; Writing – Original Draft, N.K. and S.G.G.; Writing – Review and Editing, N.K. and S.G.G.; Funding Acquisition, S.G.G. and J.Z.N.; Supervision, S.G.G.

DECLARATION OF INTERESTS

The authors declare no competing interests.

Received: January 28, 2018
Revised: September 24, 2018
Accepted: October 24, 2018
Published: November 20, 2018

REFERENCES

Akay, A., Di Domenico, T., Suen, K.M., Nabih, A., Parada, G.E., Larance, M., Medhi, R., Berkyurek, A.C., Zhang, X., Wedeles, C.J., et al. (2017). The helicase aquarius/EMB-4 is required to overcome intronic barriers to allow nuclear RNAi pathways to heritably silence transcription. Dev. Cell *42*, 241–255.e6.

Alcazar, R.M., Lin, R., and Fire, A.Z. (2008). Transmission dynamics of heritable silencing induced by double-stranded RNA in *Caenorhabditis elegans*. Genetics *180*, 1275–1288.

Andersen, E.C., and Horvitz, H.R. (2007). Two *C. elegans* histone methyltransferases repress *lin-3*EGF transcription to inhibit vulval development. Development *134*, 2991–2999.

Arribere, J.A., Bell, R.T., Fu, B.X., Artiles, K.L., Hartman, P.S., and Fire, A.Z. (2014). Efficient marker-free recovery of custom genetic modifications with CRISPR/Cas9 in *Caenorhabditis elegans*. Genetics *198*, 837–846.

Ashe, A., Sapetschnig, A., Weick, E.M., Mitchell, J., Bagijn, M.P., Cording, A.C., Doebley, A.L., Goldstein, L.D., Lehrbach, N.J., Le Pen, J., et al. (2012). piRNAs can trigger a multigenerational epigenetic memory in the germline of *C. elegans*. Cell *150*, 88–99.

Bagijn, M.P., Goldstein, L.D., Sapetschnig, A., Weick, E.M., Bouasker, S., Lehrbach, N.J., Simard, M.J., and Miska, E.A. (2012). Function, targets, and evolution of *Caenorhabditis elegans* piRNAs. Science *337*, 574–578.

Brenner, S. (1974). The genetics of *Caenorhabditis elegans*. Genetics *77*, 71–94.

Buckley, B.A., Burkhart, K.B., Gu, S.G., Spracklin, G., Kershner, A., Fritz, H., Kimble, J., Fire, A., and Kennedy, S. (2012). A nuclear Argonaute promotes multigenerational epigenetic inheritance and germline immortality. Nature *489*, 447–451.

Burkhart, K.B., Guang, S., Buckley, B.A., Wong, L., Bochner, A.F., and Kennedy, S. (2011). A pre-mRNA-associating factor links endogenous siRNAs to chromatin regulation. PLoS Genet. *7*, e1002249.

Burton, N.O., Burkhart, K.B., and Kennedy, S. (2011). Nuclear RNAi maintains heritable gene silencing in *Caenorhabditis elegans*. Proc. Natl. Acad. Sci. USA *108*, 19683–19688.

C. elegans Deletion Mutant Consortium (2012). Large-scale screening for targeted knockouts in the *Caenorhabditis elegans* genome. G3 (Bethesda) *2*, 1415–1425.

Elbashir, S.M., Lendeckel, W., and Tuschl, T. (2001). RNA interference is mediated by 21- and 22-nucleotide RNAs. Genes Dev. *15*, 188–200.

Fire, A., Xu, S., Montgomery, M.K., Kostas, S.A., Driver, S.E., and Mello, C.C. (1998). Potent and specific genetic interference by double-stranded RNA in *Caenorhabditis elegans*. Nature *391*, 806–811.

Frøkjær-Jensen, C., Jain, N., Hansen, L., Davis, M.W., Li, Y., Zhao, D., Rebora, K., Millet, J.R.M., Liu, X., Kim, S.K., et al. (2016). An abundant class of non-coding DNA can prevent stochastic gene silencing in the *C. elegans* germline. Cell *166*, 343–357.

Garrigues, J.M., Sidoli, S., Garcia, B.A., and Strome, S. (2015). Defining heterochromatin in *C. elegans* through genome-wide analysis of the heterochromatin protein 1 homolog HPL-2. Genome Res. *25*, 76–88.

Gaydos, L.J., Rechtsteiner, A., Egelhofer, T.A., Carroll, C.R., and Strome, S. (2012). Antagonism between MES-4 and Polycomb repressive complex 2 promotes appropriate gene expression in *C. elegans* germ cells. Cell Rep. *2*, 1169–1177.

Greer, E.L., Beese-Sims, S.E., Brookes, E., Spadafora, R., Zhu, Y., Rothbart, S.B., Aristizábal-Corrales, D., Chen, S., Badeaux, A.I., Jin, Q., et al. (2014). A histone methylation network regulates transgenerational epigenetic memory in *C. elegans*. Cell Rep. *7*, 113–126.

Grishok, A., Tabara, H., and Mello, C.C. (2000). Genetic requirements for inheritance of RNAi in *C. elegans*. Science *287*, 2494–2497.

Gu, S.G., Pak, J., Guang, S., Maniar, J.M., Kennedy, S., and Fire, A. (2012). Amplification of siRNA in *Caenorhabditis elegans* generates a transgenerational sequence-targeted histone H3 lysine 9 methylation footprint. Nat. Genet. *44*, 157–164.

Guang, S., Bochner, A.F., Burkhart, K.B., Burton, N., Pavelec, D.M., and Kennedy, S. (2010). Small regulatory RNAs inhibit RNA polymerase II during the elongation phase of transcription. Nature *465*, 1097–1101.

Hammond, S.M., Bernstein, E., Beach, D., and Hannon, G.J. (2000). An RNA-directed nuclease mediates post-transcriptional gene silencing in *Drosophila* cells. Nature *404*, 293–296.

Hammond, S.M., Boettcher, S., Caudy, A.A., Kobayashi, R., and Hannon, G.J. (2001). Argonaute2, a link between genetic and biochemical analyses of RNAi. Science *293*, 1146–1150.

Kalinava, N., Ni, J.Z., Peterman, K., Chen, E., and Gu, S.G. (2017). Decoupling the downstream effects of germline nuclear RNAi reveals that H3K9me3 is dispensable for heritable RNAi and the maintenance of endogenous siRNA-mediated transcriptional silencing in *Caenorhabditis elegans*. Epigenetics Chromatin *10*, 6.

Kelly, W.G., Xu, S., Montgomery, M.K., and Fire, A. (1997). Distinct requirements for somatic and germline expression of a generally expressed *Caernorhabditis elegans* gene. Genetics *146*, 227–238.

Kennerdell, J.R., and Carthew, R.W. (1998). Use of dsRNA-mediated genetic interference to demonstrate that frizzled and frizzled 2 act in the wingless pathway. Cell *95*, 1017–1026.

Langmead, B., Trapnell, C., Pop, M., and Salzberg, S.L. (2009). Ultrafast and memory-efficient alignment of short DNA sequences to the human genome. Genome Biol. *10*, R25.

Leopold, L.E., Heestand, B.N., Seong, S., Shtessel, L., and Ahmed, S. (2015). Lack of pairing during meiosis triggers multigenerational transgene silencing in *Caenorhabditis elegans*. Proc. Natl. Acad. Sci. USA *112*, E2667–E2676.

Lev, I., Seroussi, U., Gingold, H., Bril, R., Anava, S., and Rechavi, O. (2017). MET-2-dependent H3K9 methylation suppresses transgenerational small RNA inheritance. Curr. Biol. *27*, 1138–1147.

Lin, R. (2003). A gain-of-function mutation in oma-1, a *C. elegans* gene required for oocyte maturation, results in delayed degradation of maternal proteins and embryonic lethality. Dev. Biol. *258*, 226–239.

Mao, H., Zhu, C., Zong, D., Weng, C., Yang, X., Huang, H., Liu, D., Feng, X., and Guang, S. (2015). The Nrde pathway mediates small-RNA-directed histone H3 lysine 27 trimethylation in *Caenorhabditis elegans*. Curr. Biol. *25*, 2398–2403.

Martienssen, R., and Moazed, D. (2015). RNAi and heterochromatin assembly. Cold Spring Harb. Perspect. Biol. *7*, a019323.

McMurchy, A.N., Stempor, P., Gaarenstroom, T., Wysolmerski, B., Dong, Y., Aussianikava, D., Appert, A., Huang, N., Kolasinska-Zwierz, P., Sapetschnig, A., et al. (2017). A team of heterochromatin factors collaborates with small RNA pathways to combat repetitive elements and germline stress. eLife *6*, e21666.

Minkina, O., and Hunter, C.P. (2017). Stable heritable germline silencing directs somatic silencing at an endogenous locus. Mol. Cell *65*, 659–670.e5.

Ni, J.Z., Chen, E., and Gu, S.G. (2014). Complex coding of endogenous siRNA, transcriptional silencing and H3K9 methylation on native targets of germline nuclear RNAi in *C. elegans*. BMC Genomics *15*, 1157.

Ni, J.Z., Kalinava, N., Chen, E., Huang, A., Trinh, T., and Gu, S.G. (2016). A transgenerational role of the germline nuclear RNAi pathway in repressing heat stress-induced transcriptional activation in *C. elegans*. Epigenetics Chromatin *9*, 3.

Paix, A., Folkmann, A., Rasoloson, D., and Seydoux, G. (2015). High efficiency, homology-directed genome editing in *Caenorhabditis elegans* using CRISPR-Cas9 ribonucleoprotein complexes. Genetics *201*, 47–54.

Pak, J., and Fire, A. (2007). Distinct populations of primary and secondary effectors during RNAi in *C. elegans*. Science *315*, 241–244.

Pezic, D., Manakov, S.A., Sachidanandam, R., and Aravin, A.A. (2014). piRNA pathway targets active LINE1 elements to establish the repressive H3K9me3 mark in germ cells. Genes Dev. *28*, 1410–1428.

Shirayama, M., Seth, M., Lee, H.C., Gu, W., Ishidate, T., Conte, D., Jr., and Mello, C.C. (2012). piRNAs initiate an epigenetic memory of nonself RNA in the *C. elegans* germline. Cell *150*, 65–77.

Sienski, G., Dönertas, D., and Brennecke, J. (2012). Transcriptional silencing of transposons by Piwi and maelstrom and its impact on chromatin state and gene expression. Cell *151*, 964–980.

Sijen, T., Steiner, F.A., Thijssen, K.L., and Plasterk, R.H. (2007). Secondary siRNAs result from unprimed RNA synthesis and form a distinct class. Science *315*, 244–247.

Spracklin, G., Fields, B., Wan, G., Vijayendran, D., Wallig, A., Shukla, A., and Kennedy, S. (2017). Identification and characterization of *Caenorhabditis elegans* RNAi inheritance machinery. Genetics, Published online May 22, 2017. https://doi.org/10.1534/genetics.116.198812.

Timmons, L., Court, D.L., and Fire, A. (2001). Ingestion of bacterially expressed dsRNAs can produce specific and potent genetic interference in *Caenorhabditis elegans*. Gene *263*, 103–112.

Towbin, B.D., González-Aguilera, C., Sack, R., Gaidatzis, D., Kalck, V., Meister, P., Askjaer, P., and Gasser, S.M. (2012). Step-wise methylation of histone H3K9 positions heterochromatin at the nuclear periphery. Cell *150*, 934–947.

Tuschl, T., Zamore, P.D., Lehmann, R., Bartel, D.P., and Sharp, P.A. (1999). Targeted mRNA degradation by double-stranded RNA in vitro. Genes Dev. *13*, 3191–3197.

Vastenhouw, N.L., Brunschwig, K., Okihara, K.L., Müller, F., Tijsterman, M., and Plasterk, R.H. (2006). Gene expression: long-term gene silencing by RNAi. Nature *442*, 882.

Wassenegger, M. (2000). RNA-directed DNA methylation. Plant Mol. Biol. *43*, 203–220.

Weiser, N.E., Yang, D.X., Feng, S., Kalinava, N., Brown, K.C., Khanikar, J., Freeberg, M.A., Snyder, M.J., Csankovszki, G., Chan, R.C., et al. (2017). MORC-1 integrates nuclear RNAi and transgenerational chromatin architecture to promote germline immortality. Dev. Cell *41*, 408–423.e7.

Woodhouse, R.M., Buchmann, G., Hoe, M., Harney, D., Larance, M., Boag, P.R., and Ashe, A. (2018). The chromatin modifiers SET-25 and SET-32 are required for initiation but not long-term maintenance of transgenerational epigenetic inheritance. Cell Reports *25*, this issue, 2259–2272.

STAR★METHODS

KEY RESOURCES TABLE

REAGENT or RESOURCE	SOURCE	IDENTIFIER
Antibodies		
Anti-Histone H3 (tri methyl K9) antibody - ChIP Grade	Abcam	Cat# 8898, Lot# GR285794-2; RRID: AB_306848
Anti-RNA polymerase II CTD repeat YSPTSPS (phospho S2) antibody - ChIP Grade	Abcam	Cat# ab5095, Lot# GR231750-1; RRID: AB_304749
Bacterial and Virus Strains		
E. coli OP50	CGC	NA
E. coli HT115(DE3)	CGC	NA
Chemicals, Peptides, and Recombinant Proteins		
FORMALDEHYDE 37% MICROFILTERED	Electron Microscopy Sciences	Cat# 15686
TRIzol-REAGENT	Invitrogen	Cat# 15596-018
RNA Fragmentation Reagents	Invitrogen	Cat# AM8740
T4 PNK	NEB	Cat# M0201L
T4 RNA Ligase 1	NEB	Cat# M0204S
T4 RNA ligase 2, truncated	NEB	Cat# M0242L
Critical Commercial Assays		
KAPA Hyper Prep Kit	KAPABIOSYSTEM	Cat# KK8505
KAPA SYBR FAST Universal 2 × PCR Master Mix	KAPABIOSYSTEM	Cat# KK4602
Deposited Data		
NGS data	This study	NGS: GSE117662
Experimental Models: Organisms/Strains		
C. elegans Bristol strain	CGC	N2
set-32(ok1457) I	(*C. elegans* Deletion Mutant Consortium, 2012)	VC967
set-32(red11) I	This study	CSS186
nrde-2(gg091) II	(Guang et al., 2010)	YY186
met-2(n4256) III	(Andersen and Horvitz, 2007)	MT13293
hrde-1(tm1200) III	(*C. elegans* Deletion Mutant Consortium, 2012)	TM1300
set-25(n5021) III	(Andersen and Horvitz, 2007)	MT17463
set-26(tm3526) IV	(*C. elegans* Deletion Mutant Consortium, 2012)	TM3526
set-9(red8) IV	(Kalinava et al., 2017)	CSS164
set-26(tm3526) set-9(red8)	this study	CSS412
set-32(red11); hrde-1(tm1200)	this study	CSS425
met-2(n4256) set-25(n5021)	(Kalinava et al., 2017)	CSS95
set-32(red11);met-2(n4256) set-25(n5021)	(Kalinava et al., 2017)	CSS419
met-2(n4256) set-25(n5021) hrde-1(tm1200)	this study	CSS400
set-32(red11);met-2(n4256) set-25(n5021) hrde-1(tm1200)	this study	CSS415
Oligonucleotides		
forward qPCR primer for oma-1 mRNA: ctacaggactctgcccatacg	IDT	SG-1016
reverse qPCR primer for oma-1 mRNA: ggcctggcaaacatttctaa	IDT	SG-1019
forward qPCR primer for oma-1 pre-mRNA:ttaatgacc tctgttttaggtg	IDT	SG-1022
reverse qPCR primer for oma-1 pre-mRNA:gaacccaaaa ccatcgaatc	IDT	SG-1023

(*Continued on next page*)

Continued		
REAGENT or RESOURCE	SOURCE	IDENTIFIER
forward qPCR primer for oma-1 ChIP: acatgtatttttgctcactgtaa	IDT	SG-1018
reverse qPCR primer for oma-1 ChIP: ggcctggcaaacatttctaa	IDT	SG-1019
forward ChIP qPCR primer for an H3K9me3 negative control locus: agccatggcacaaaaagaag	IDT	SG-1044
reverse ChIP qPCR primer for an H3K9me3 negative control locus: tgtggcctgagaagacaaaa	IDT	SG-1045
forward qPCR primer for tba-1 mRNA: TCCAAGCGAG ACCAGGCTTCAG	IDT	SG-1108
reverse qPCR primer for tba-1 mRNA: TCAACACTGCCAT CGCCGCC	IDT	SG-1109
HR oligo for set-32 (red11) CRISPR allele): tcttcgaatatacagacacg aatgttttgaacccgGCTAGCAtgctccgcaagaaacattgcgaaagcatgta ttatgtctcaaaaggaagagaat	IDT	SG-1173
T7 *in vitro* transcription template oligo for crRNA targeting hrde-1 tm1200 mutation (seed sequence: taatcgtatgTggaaaccg): AAAACAGCATAGCTCTAAAAC cggtttccAcatacgatta CCCTATAGTGAGTCGTATTA	IDT	SG-1285
upstream PCR primer used to generated a 424 bp genomic DNA fragment as template DNA to repair the hrde-1(tm1200) mutation by CRISPR: aaggagaagttgcccaggag	IDT	SG-1292
downstream PCR primer used to generated a 424 bp genomic DNA fragment as template DNA to repair the hrde-1(tm1200) mutation by CRISPR: atctcggtacctgtcgttgc	IDT	SG-1293
Recombinant DNA		
oma-1 dsRNA feeding plasmid	(Kalinava et al., 2017)	pSG42
Software and Algorithms		
Bowtie 0.12.7	(Langmead et al., 2009)	NA

CONTACT FOR REAGENT AND RESOURCE SHARING

Requests and further information for reagents and resources should be directed to and will be fulfilled by the Lead Contact, Sam G. Gu (sam.gu@rutegers.edu).

EXPERIMENTAL MODEL AND SUBJECT DETAILS

All *C.elegans* strains used in this study are listed in Key Resources Table. *C. elegans* was cultured with OP50 *E. coli* as the food source for all non-RNAi experiments (Brenner, 1974). Worms were cultured at 20°C for all of the experiments conducted in this study. Synchronized young adult animals were ground in liquid nitrogen by mortar and pestle and stored at −80°C and used for all data analysis. Experiments involving WT and mutant *C. elegans* are approved by Rutgers Environmental Health and Safety under "recombinant DNA" protocol.

METHOD DETAILS

oma-1 RNAi experiments

oma-1 RNAi experiments were performed as described previously (Kalinava et al., 2017; Timmons et al., 2001) with the following modifications. Two schemes of *oma-1* RNAi were used in this study. To examine the onset of RNAi, synchronized L1 larvae were released onto *oma-1* RNAi plates which contained *oma-1*-dsRNA-expressing *E. coli*. The young adult animals are referred to as F1(dsRNA$^+$). To obtain worms of F2(dsRNA$^+$) or with extended generations of dsRNA exposure, eggs from dsRNA$^+$ adult animals were collected and hatched in M9 buffer. L1s were released onto *oma-1* RNAi plates for another generation of dsRNA exposure. Young adult animals (59-60 hours after L1 release at 20°C, before egg laying starts, but embryos are visible inside the uterus) were harvested for various assays throughout the experiments. For the *oma-1* heritable RNAi and H3K9me3 ChIP experiments in Figure S2, worms of mixed developmental stages were first cultured on *oma-1* RNAi plates continuously for 9-10 days starting with approximately 5 L3-L4 worms, followed by one round of synchronized culture on *oma-1* RNAi plates to collect young adults. Samples used in the same figure panel were prepared in parallel.

Gene conversion to repair hrde-1 mutation using CRISPR-Cas9

We repaired the *hrde-1(tm1200)* mutation to the WT sequence by injecting a plasmid Cas9 plasmid and hrde-1-targeting a *hrde-1* targeting Cas-9 ribonuclease complex and PCR fragment as the repair template. A *dpy-10(cn64)* co-conversion marker was used (Arribere et al., 2014; Paix et al., 2015). 10-15 adult hermaphrodite animals (P0s) of each strain were injected. We screened 48-96 F1s animals using single-worm PCR from broods of injected animals with high frequencies of roller F1s. This yielded with 2-8 F1s bearing potential gene conversion events (heterozygotes) identified by the size of PCR products. For each putative F1 hit, 12-24 F2 worms a WT copy of *dpy-10* were individually transferred to plates. After laying eggs, the F2 worms with homozygous WT *hrde-1* sequences were identified by PCR and Sanger sequencing. We refer to the CRISPR/Cas-9-generated WT *hrde-1* sequence as *hrde-1(+^{R})* to distinguish it from the naive WT *hrde-1* sequence, referred to as *hrde-1(+).* F3, F4, F5, F10, and F20 post-conversion adults were collected either by hand picking (F3 and F4) or synchronized culture (F5 and later generations). The control *hrde-1(+)* samples (WT, *set-32*, *met-2 set-25*, *set-32; met-2 set-25)* and *hrde-1(-)* samples (*hrde-1*, *set-32; hrde-1*, *met-2 set-25 hrde-1* and *set-32; met-2 set-25 hrde-1)* were collected by picking adult animals, identically to the F3 and F4 samples of the *hrde-1(+^{R})* samples.

Total RNA extraction

For samples of pooled whole worms, TRIzol reagent (Life Technologies) was added to the frozen sample of approximately 20 worms in the M9 buffer. To ensure break down of worm bodies, we used 3-4 cycles of freeze-thawing in TRIzol, then performed total RNA extraction according to the manufacture's protocol. This procedure yielded 1-3 μg of total RNA for each sample.

mRNA and pre-mRNA RT-qPCR

Total RNA extraction was performed using the TRIzol Reagent. 1 μg of total RNA was used for the first strand cDNA synthesis with SuperScript III RT kit (Life Technologies) and oligo-dT as the primer for mRNA RT-qPCR and the random hexamers as the primer mix for pre-mRNA RT-qPCR.

qPCR was performed using KAPA SYBR FAST Universal 2 × PCR Master Mix (KAPA Biosystems) on a Mastercycler EP Realplex realtime PCR system (Eppendorf) according to the manufacturer's instructions. qPCR primers are listed in Key Resources Table. Each sample was processed in triplicate. Reported values for the fold change of mRNA and pre-mRNA were calculated using ΔΔCT analysis. *tba-1* was used as a reference gene.

High-throughput sequencing

Chromatin immunoprecipitation (ChIP): Pol II and H3K9me3 ChIP-seq was performed as described previously (Ni et al., 2014). The anti-RNA Pol II S2 antibody (ab5095, Abcam) and anti-H3K9me3 antibody (ab8898, Abcam) were used.

RNA-seq: Ribosomal RNA (rRNA) was removed from the total RNA using RNase H and anti-rRNA oligo mixture (total of 110, listed in Table S1). The rRNA-removal procedure was adopted from (Frøkjær-Jensen et al., 2016). Briefly 1.25 μg of anti-rRNA oligos were mixed with 0.5 μg total RNA in 1x Hybridization Buffer (100 mM Tris-HCl pH 7.4, 200mM NaCl) in a final volume of 8 μl. The sample was denatured at 95°C for 2 minutes, and then cooled at −0.1°C /sec to 45°C. Equal volumes of Hybridase Thermostable RNase H (5U/μl,Epicenter) and 10x RNaseH Reaction Buffer (500 mM Tris-HCl pH 7.4, 1 M NaCl, 200 mM $MgCl_2$) were mixed and preheated to 45°C before use. 2 μl of the enzyme mix was added to each reaction mix, which was then incubated at 45°C for 1 hr. To remove DNA oligos, 5 μl TURBO DNase buffer, 3 μl TURBO DNase (Invitrogen), and 32 μl diH2O were added to the reaction mix, followed by 37°C incubation for 30 minutes. To purify RNA, 300 μl STOP solution (1 M ammonium acetate, 10 mM EDTA) was added to the reaction mix, followed by phenol/chloroform (1:1) extraction and ethanol precipitation. The resulting RNA (without poly(A) selection) was used to prepare the RNA-seq library as described previously (Ni et al., 2014).

siRNA-seq: small RNA isolation and RNA-seq library construction were performed as described previously (Ni et al., 2014).

All libraries were sequenced using Illumina HiSeq 2500 platform, with a 50-nt single-end run and dedicated index sequencing. All libraries used in this study are listed in Table S2.

QUANTIFICATION AND STATISTICAL ANALYSIS

Whole genome alignment of the sequencing reads to the *C. elegans* genome (WS190 version) was done using Bowtie (0.12.7) (Langmead et al., 2009). Only perfectly aligned reads were used for data analysis. Reads that aligned to N different loci were scaled by a factor of 1/N. Custom R and python scripts were used in this study. Normalization based on total reads aligned to the whole genome for each library was used for all data analysis, except for the ΔPol II boxplot analysis in Figure S9C, where total reads count of the top 5th percentile of the Pol II signal in corresponding library was used as the normalization factor. The three-region Venn diagram was generated using a web-based software (http://www.benfrederickson.com/venn-diagrams-with-d3.js/). Wilcoxon signed-rank test was performed to calculate the p values for all box-plot analysis in Figures 3E, S9C, and S9D. Welch Two Sample t test was used to calculate all other p values.

DATA AND SOFTWARE AVAILABILITY

The accession number for the raw sequencing data in the fastq format reported in this paper is NCBI GEO: GSE117662.

Cell Reports, Volume *25*

Supplemental Information

C. elegans Heterochromatin Factor SET-32 Plays an Essential Role in Transgenerational Establishment of Nuclear RNAi-Mediated Epigenetic Silencing

Natallia Kalinava, Julie Zhouli Ni, Zoran Gajic, Matthew Kim, Helen Ushakov, and Sam Guoping Gu

Fig. S1-S9

Supplemental figure 1

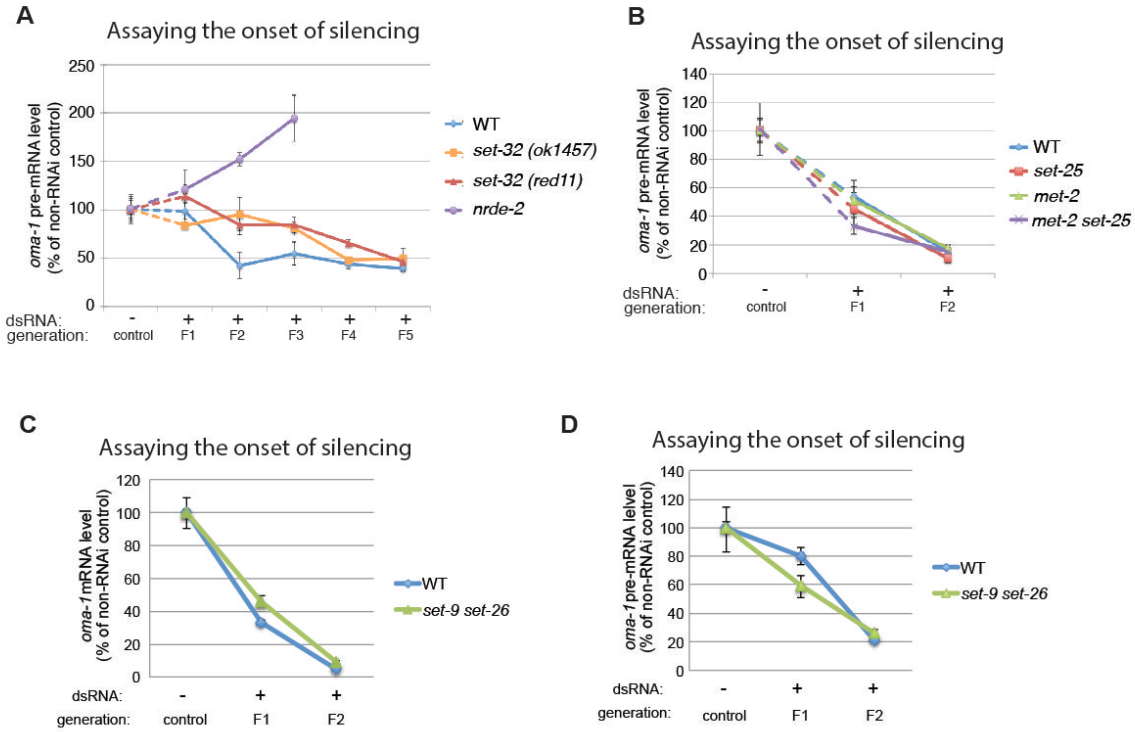

Figure S1. Multigenerational analysis of dsRNA-triggered RNAi at *oma-1*. Related to Figure 1. (A) RT-qPCR analysis of *oma-1* pre-mRNA of the control samples and F1-F5(dsRNA+) samples for wild type and two different *set-32* mutant strains, and F1-F3(dsRNA+) samples for *nrde-2* mutant. The WT and *set-32* results are the second biological replicate of the experiment shown in Fig. 1C. (B) RT-qPCR analysis of *oma-1* pre-mRNA of the control samples and F1-F2(dsRNA+) samples for WT, *met-2, set-25*, and *met-2 set-25* mutant strains. (C-D) RT-qPCR analysis of *oma-1* mRNA (C) and pre-mRNA (D) of the control samples and F1-F2(dsRNA+) samples for WT and *set-9 set-26 double* mutant strains. Samples for each panel were collected in parallel. Each RT-qPCR value in this figure represent the mean value of n=3, whiskers represent the SD.

Supplemental figure 2

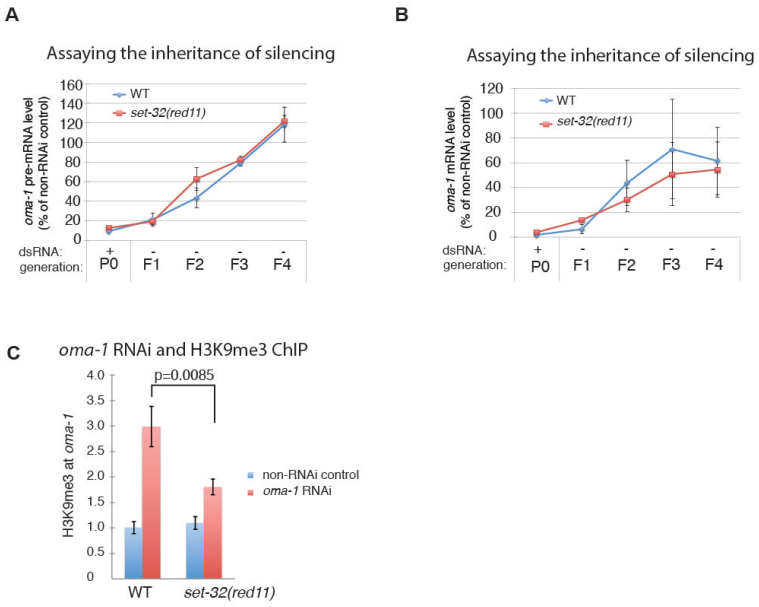

Figure S2. Characterization of the *set-32(red11)* mutant strain. Related to Figure 1. (A and B) Heritable RNAi assay using *oma-1* as the target gene. P0: a population cultured on *oma-1* dsRNA-expressing *E. coli* for approximately 4 generations. F1-F4 progeny of P0 were cultured in the absence of *oma-1* dsRNA. Synchronized adults were collected for all samples. *oma-1* pre-mRNA (A) and mRNA (B) levels were examined by RT-qPCR. Values are expressed as percentage of RNA expression in the non-RNAi control sample of the same genotype. (C) H3K9me3 ChIP-qPCR analysis to examine the dsRNA-induced H3K9me3 at *oma-1* in WT and *set-32(red11)* mutant. OP50-fed adults (control) and adult animals from a population with 4-5 generation *oma-1* dsRNA feeding were used in this assay. Each RT-qPCR value in this figure represent the mean value of n=3, whiskers represent the SD. Welch Two Sample t-test was used to calculate p-value in (C).

Supplemental figure 3

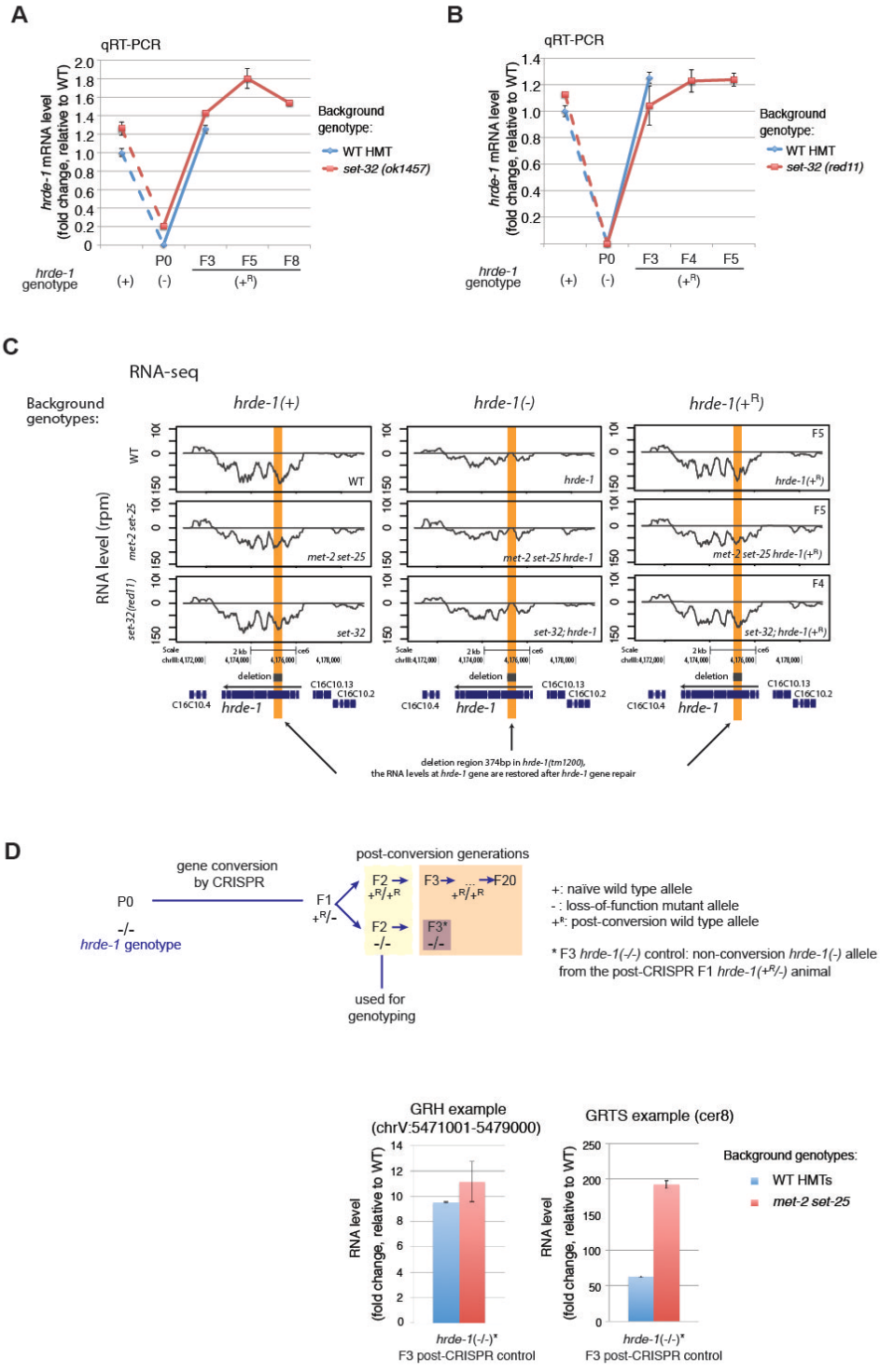

Figure S3. Examining the *hrde-1* mRNA expression in the silencing establishment assay. Related to Figure 2. (A and B) RT-qPCR analysis of *hrde-1* mRNA using primers that are located within the deleted sequence in the *hrde-1(tm1200)* mutation. (C) RNA-seq profiles at the *hrde-1* locus. The *hrde-1(tm1200)* deletion is marked by an orange stripe. Each RNA-seq profile is normalized by total reads aligned to the whole genome. (D) The *hrde-1*(-/-) progeny (F3) from the *hrde-1*(-/+^{R}) (F1) were collected for RT-qPCR analysis. This was done for both wild type HMT and *met-2 set-25* mutant backgrounds. The RNA levels in (A), (B) and (D) were normalized to the one of *hrde-1*(+/+) populations. Each RT-qPCR value in (A), (B) and (D) represent the mean value of n=3, whiskers represent the SD.

Supplemental figure 4

A control region that includes an actively expressed gene *cdc-42*. (chrII:7613000-7623000)

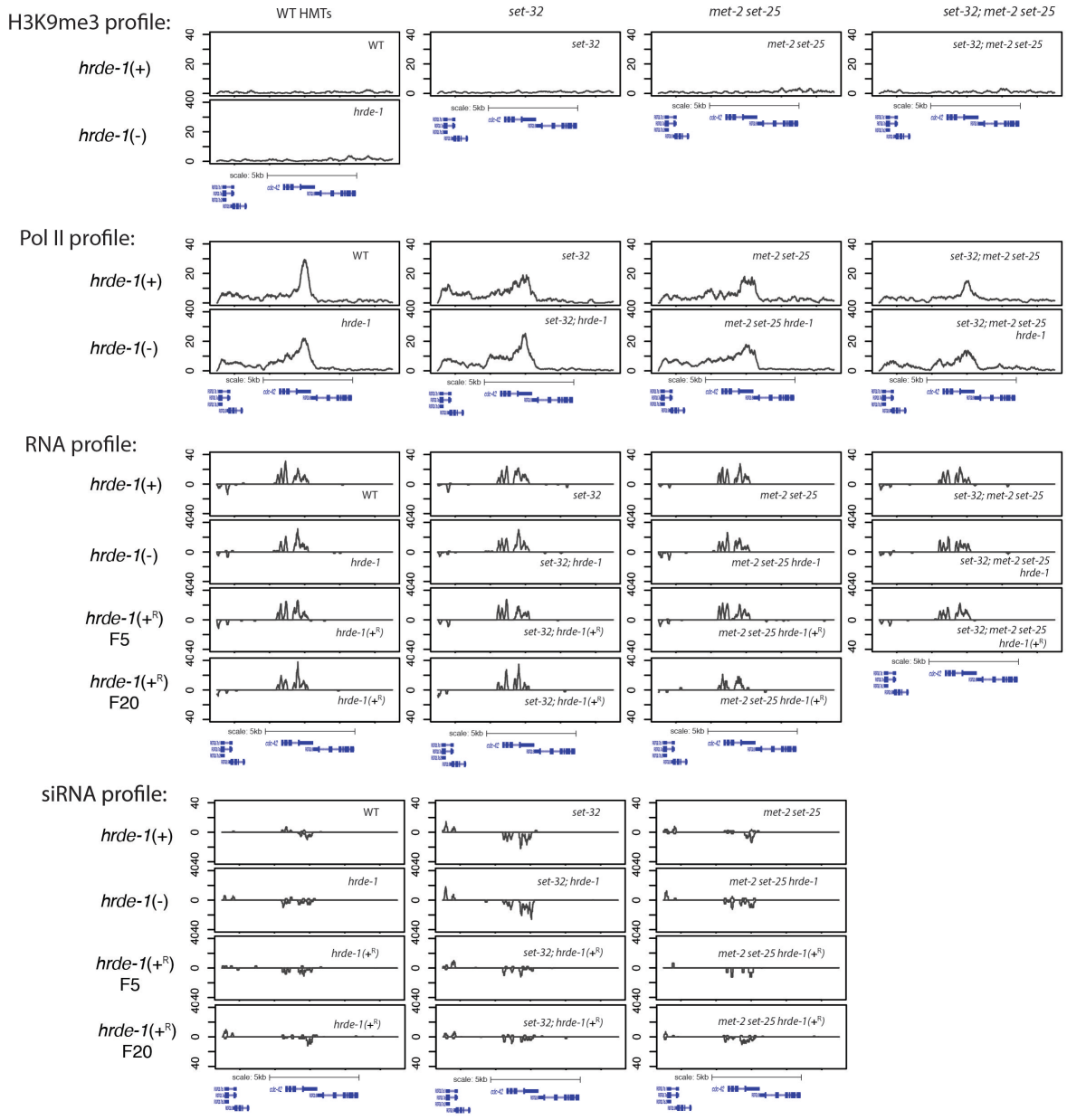

Figure S4. ChIP-seq (H3K9me3 and RNA Pol II [S2 phosphorylated]) and RNA-seq (rRNA-removed) and sRNA-seq profiles at *cdc-42* (a control region, no nuclear RNAi activity). Related to Figure 3. The H3K9me3 ChIP-seq data were from our previous study (Kalinava et al., 2017) and the rest of the data were generated in this study. For total RNA and sRNA-seq, the coverages of the "+" and "-"-strand reads are separately plotted ("+": above the 0-horizontal line, "-": below). Each profile is normalized by total reads aligned to the whole genome.

Supplemental figure 5

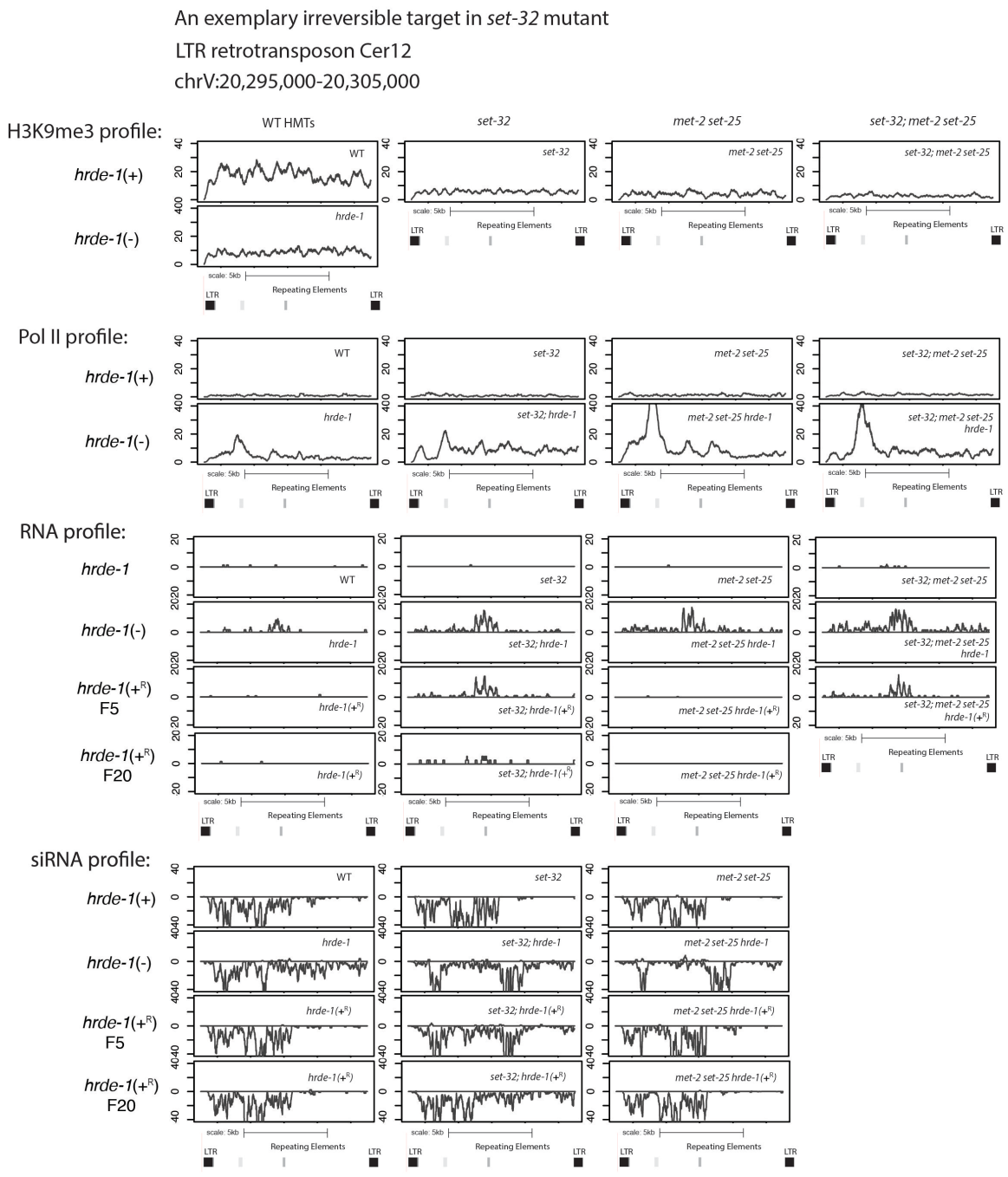

Figure S5. An exemplary irreversible target with delayed silencing establishment in *set-32;hrde-1(+^{R})*, LTR retrotransposon Cer12. Related to Figure 3. The H3K9me3 ChIP-seq data were from our previous study (Kalinava et al., 2017) and the rest of the data were generated in this study. For total RNA and sRNA-seq, the coverages of the "+" and "-"-strand reads are separately plotted ("+": above the 0-horizontal line, "-": below). Each profile is normalized by total reads aligned to the whole genome.

Supplemental figure 6

An exemplary irreversible target in *set-32* mutant (*f15d4.5 and f15d4.6*).
chrII:13240000-13255000

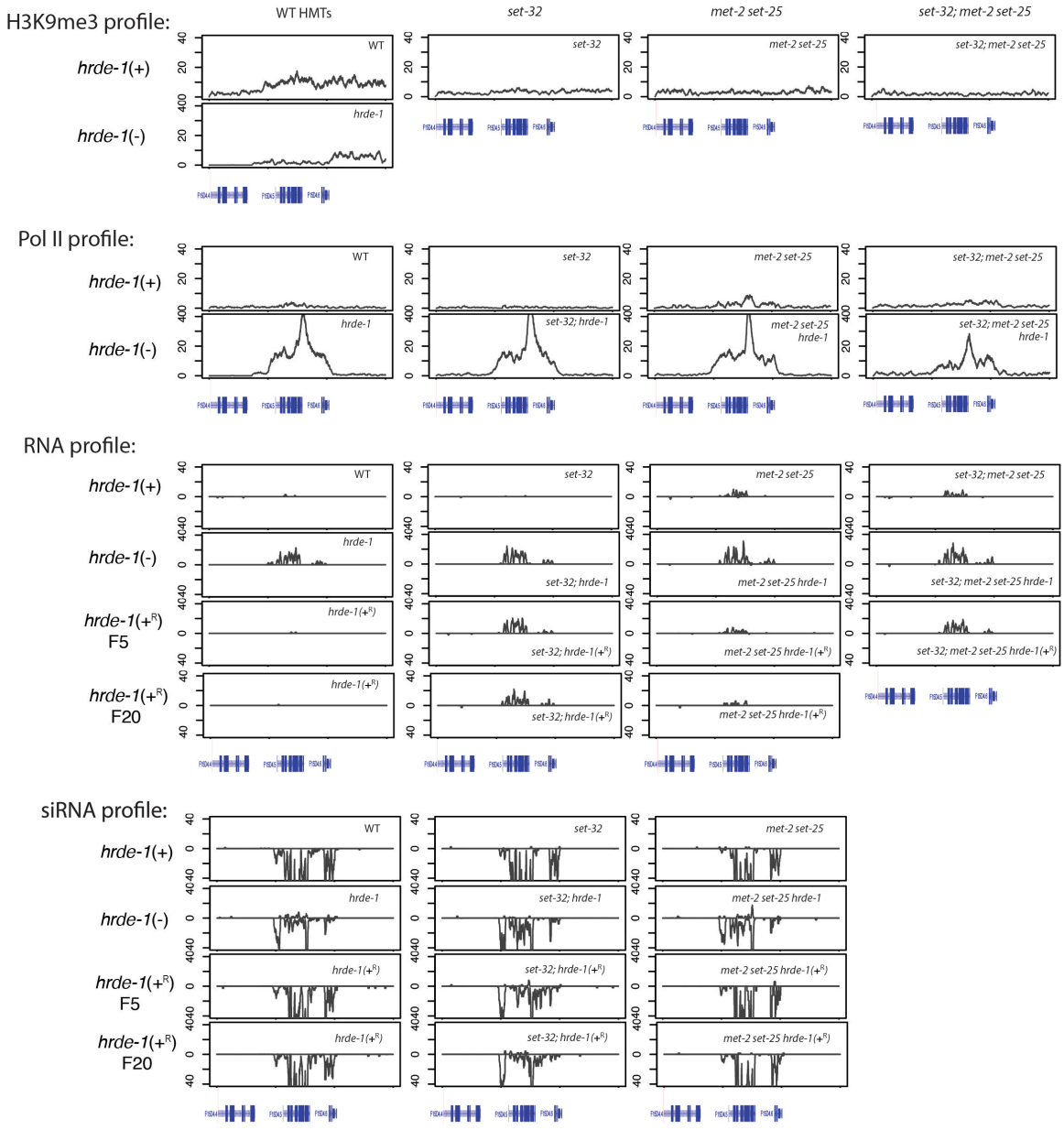

Figure S6. An exemplary irreversible target with delayed silencing establishment in *set-32;hrde-1(+^{R})*, a locus containing *f15d4.5* and *f15d4.6*. Related to Figure 3. The H3K9me3 ChIP-seq data were from our previous study (Kalinava et al., 2017) and the rest of the data were generated in this study. For total RNA and sRNA-seq, the coverages of the "+" and "-"-strand reads are separately plotted ("+": above the 0-horizontal line, "-": below). Each profile is normalized by total reads aligned to the whole genome.

Supplemental figure 7

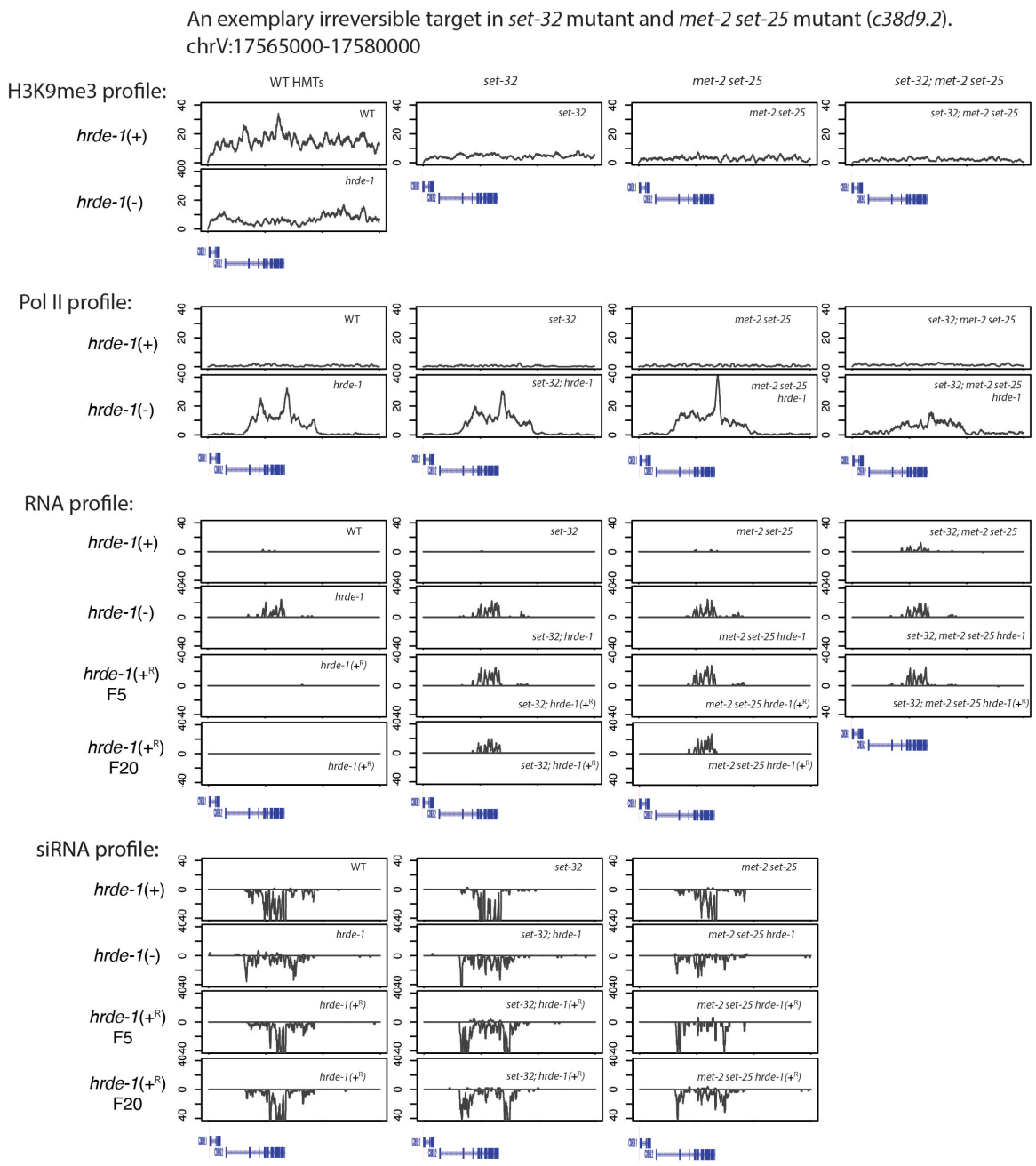

Figure S7. An exemplary irreversible target with delayed silencing establishment in *set-32;hrde-1(+^{R})*, *c38d9.2*. Related to Figure 3. The H3K9me3 ChIP-seq data were from our previous study (Kalinava et al., 2017) and the rest of the data were generated in this study. For total RNA and sRNA-seq, the coverages of the "+" and "-"-strand reads are separately plotted ("+": above the 0-horizontal line, "-": below). Each profile is normalized by total reads aligned to the whole genome.

Supplemental figure 8

An exemplary irreversible target in *set-32* mutant (LTR retrotransposon Cer9).
chrV:8865000-8890000

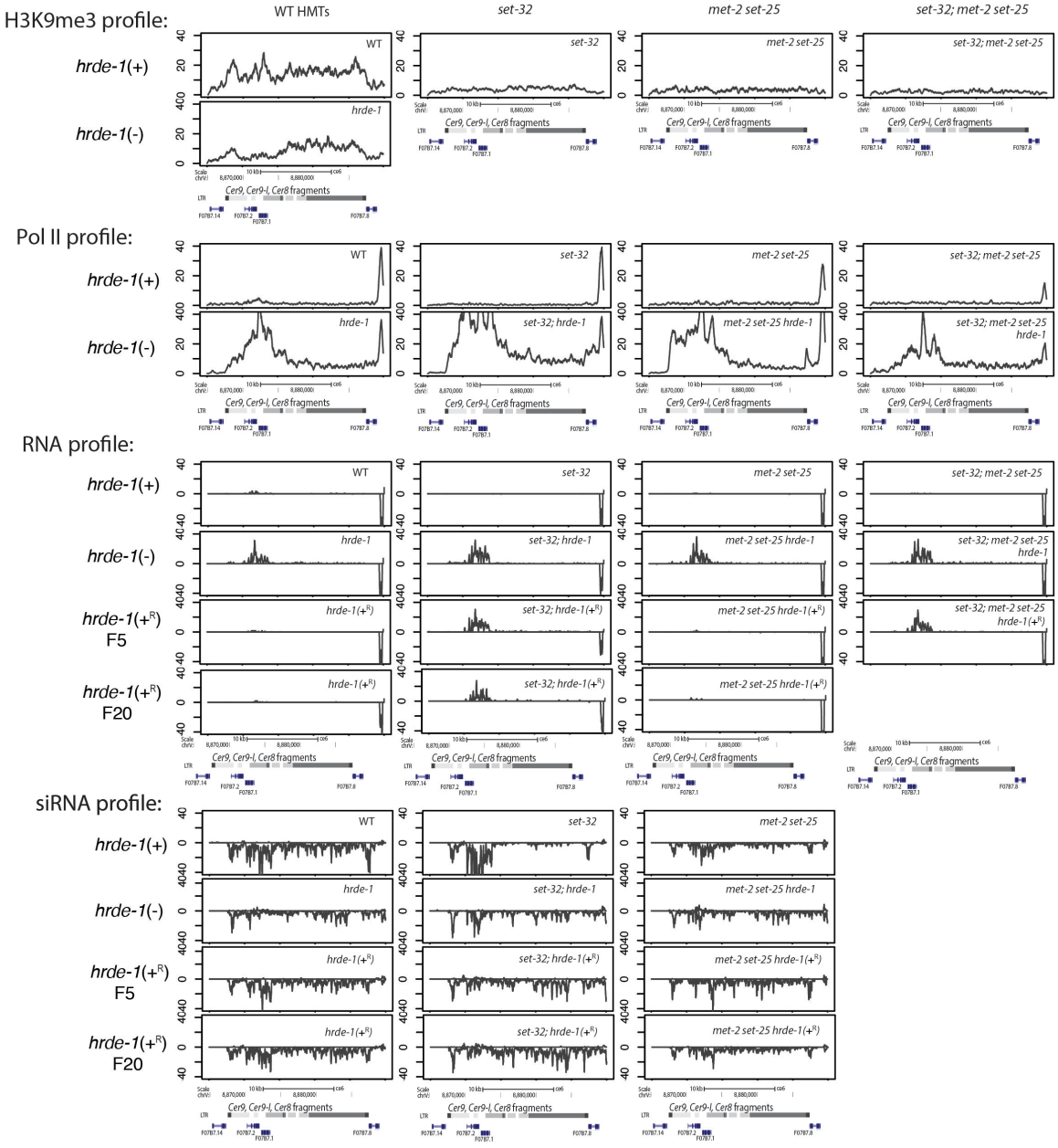

Figure S8. An exemplary irreversible target with delayed silencing establishment in *set-32;hrde-1(+^{R}),* LTR retrotransposon Cer9. Related to Figure 3. Some of the coverage plots in Fig. S8 were also presented in Figure 3. The H3K9me3 ChIP-seq data were from our previous study (Kalinava et al., 2017) and the rest of the data were generated in this study. For total RNA and sRNA-seq, the coverages of the "+" and "-"-strand reads are separately plotted ("+": above the 0-horizontal line, "-": below). Each profile is normalized by total reads aligned to the whole genome.

Supplemental figure 9

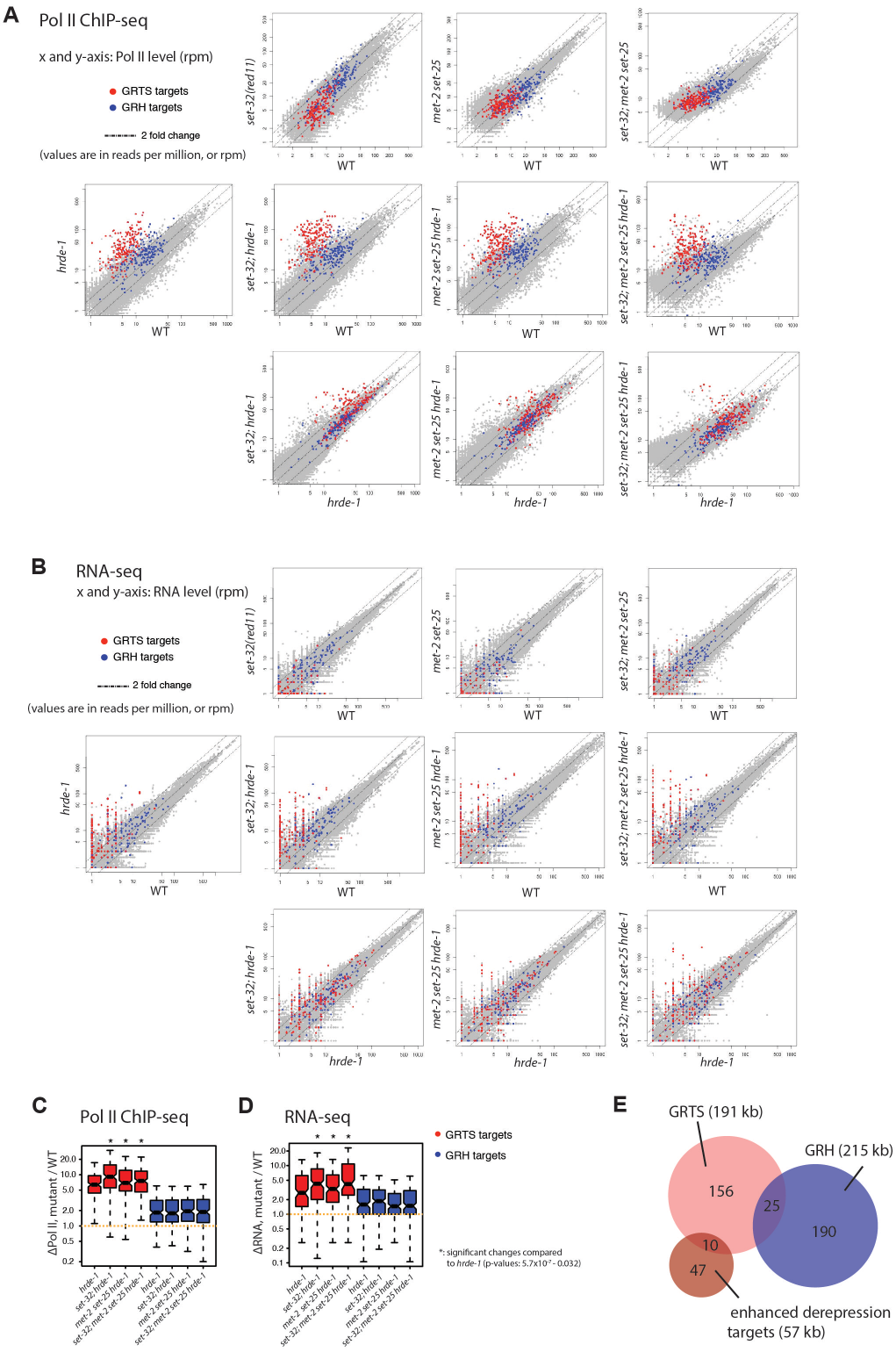

Figure S9. Whole-genome analysis of the enhancement of silencing defects caused by the combination of *H3K9 hmt* and *hrde-1* mutations. Related to Figure 4. (A and B) Scatter plot analysis of Pol II occupancy (A) and RNA expression (B) at the whole-genome level between different strains. Each dot represents a 1 kb window in the genome, normalized by total reads aligned to the whole genome. GRTS and GRH regions are highlighted as indicated. (GRTS: germline nuclear RNAi-dependent transcriptional silencing; GRH: germline nuclear RNAi-dependent heterochromatin) (C and D) Boxplot analysis of the changes in Pol II occupancy (C) and RNA expression (D) of GRTS or GRH regions between various mutants and wild type animals. Due to the skewed profile of Pol II at the low read-count region (different levels of noise at the background level), the boxplot analysis in (C) used normalization by total reads count at the top 5^{th} percentile of the Pol II signals in corresponding samples. Boxplot analysis in (D) used normalization by total reads aligned to the whole genome. (E) Venn diagram showing the relationship between GRTS, GRH, and regions with enhanced derepression in the three *H3K9 hmt;hrde-1* compound mutants.

Table S1: List of NGS libraries used in this study (NCBI GEO accession number: GSE117662). Related to Figures 1-4.

Experiment	library name
OP50 feeding, 19°C, young adults	
RNA-seq, N2	SG0117_lib1
RNA-seq, *hrde-1(tm1200)*	SG0117_lib2
RNA-seq, *set-32(ok1457)*	SG0117_lib9
RNA-seq, *set-32(red11)*	SG0117_lib5
RNA-seq, *met-2(n4256) set-25(n5021)*	SG0117_lib7
RNA-seq, *set-32(ok1457); met-2(n4256) set-25(n5021)*	SG0117_lib3
RNA-seq, *set-32(ok1457); hrde-1(tm1200)*	SG0117_lib10
RNA-seq, *set-32(red11); hrde-1(tm1200)*	SG0117_lib6
RNA-seq, *met-2(n4256) set-25(n5021) hrde-1(tm1200)*	SG0117_lib8
RNA-seq, *set-32(red11); met-2(n4256) set-25(n5021) hrde-1(tm1200)*	SG0117_lib4
Pol II ChIP-seq, N2	SG0615_lib46
Pol II ChIP-seq, *hrde-1(tm1200)*	SG0117_lib31
Pol II ChIP-seq, *set-32(red11)*	SG0117_lib27
Pol II ChIP-seq, *met-2(n4256) set-25(n5021)*	SG0615_lib50
Pol II ChIP-seq, *set-32(red11); met-2(n4256) set-25(n5021)*	SG1115_lib18
Pol II ChIP-seq, *set-32(red11); hrde-1(tm1200)*	SG0117_lib29
Pol II ChIP-seq, *met-2(n4256) set-25(n5021) hrde-1(tm1200)*	SG0615_lib8
Pol II ChIP-seq, *set-32(red11); met-2(n4256) set-25(n5021) hrde-1(tm1200)*	SG0117_lib28
siRNA-seq, N2	SG1116_lib7
siRNA-seq, *hrde-1(tm1200)*	SG0315_lib37
siRNA-seq, *set-32(ok1457)*	SG0717_lib47
siRNA-seq, *set-32(red11)*	SG0717_lib52
siRNA-seq, *met-2(n4256) set-25(n5021)*	SG0315_lib38
siRNA-seq, *set-32(ok1457); hrde-1(tm1200)*	SG0717_lib48
siRNA-seq, *set-32(red11); hrde-1(tm1200)*	SG0717_lib53
siRNA-seq, *met-2(n4256) set-25(n5021) hrde-1(tm1200)*	SG0315_lib39
***hrde-1(+R)* post-*hrde-1* repair generations, OP50 feeding, 19°C, young adults**	
RNA-seq, *hrde-1(+R)* F4	SG0117_lib14
RNA-seq, *hrde-1(+R)* F5	SG0117_lib15
RNA-seq, *hrde-1(+R)* F20	SG1217_lib7
RNA-seq, *set-32(ok1457); hrde-1(+R)* F5	SG0117_lib17
RNA-seq, *set-32(ok1457); hrde-1(+R)* F8	SG0117_lib18
RNA-seq, *set-32(ok1457); hrde-1(+R)* F20	SG1217_lib8

RNA-seq, *set-32(red11); hrde-1(+R)* F4	SG0117_lib21
RNA-seq, *set-32(red11); hrde-1(+R)* F5	SG0117_lib22
RNA-seq, *set-32(red11); hrde-1(+R)* F20	SG1217_lib9
RNA-seq, *met-2(n4256) set-25(n5021) hrde-1(+R)* F3	SG0117_lib19
RNA-seq, *met-2(n4256) set-25(n5021) hrde-1(+R)* F5	SG0117_lib20
RNA-seq, *met-2(n4256) set-25(n5021)hrde-1(+R)* F20	SG1217_lib10
RNA-seq, *set-32(red11); met-2(n4256) set-25(n5021) hrde-1(+R)* F5	SG0117_lib23
siRNA-seq, *hrde-1(+R)* F5	SG0717_lib45
siRNA-seq, *hrde-1(+R)* F20	SG0717_lib46
siRNA-seq, *set-32(ok1457); hrde-1(+R)* F8	SG0717_lib50
siRNA-seq, *set-32(ok1457); hrde-1(+R)* F20	SG0717_lib51
siRNA-seq, *set-32(red11); hrde-1(+R)* F5	SG0717_lib55
siRNA-seq, *set-32(red11); hrde-1(+R)* F20	SG0717_lib56
siRNA-seq, *met-2(n4256) set-25(n5021) hrde-1(+R)* F5	SG0717_lib58
siRNA-seq, *met-2(n4256) set-25(n5021) hrde-1(+R)* F20	SG0717_lib59
WT, oma-1 RNAi or control, 19˚C, young adults	
H3K9me3 ChIP-seq, N2, dsRNA- control	SG1217_lib43
H3K9me3 ChIP-seq, N2, oma-1 RNAi, F1	SG1217_lib44
H3K9me3 ChIP-seq, N2, oma-1 RNAi, F2	SG1217_lib45

Table S2: List of 50-nt DNA oligo sequences used for RNaseH-based rRNA depletion. Related to Figures 3-4.

Sequences:
caaaaaactcaatcaaaggatagtctcaacagatcgcagtataaaaggac
tgctctactgaatacaacaccttgaccaagagaccaagtcgtatgcaagt
gatttagcgccccgacattgaaccagagtgatctggcgttggcaagcgtc
gcagaattcactacgacgccaaggccatacatagggcataagctctcgtg
ttgccacgagatagagatgcctcccgacaccgggaagcaagaaattttcg
ccttgacaaggcgagattctaacttagaggcgttcagttataatctctca
aatggtagcttcagaccattgatctgtcgatcaagtttatgaaccaaatg
tttgaacccgctgttcctctcgtactaagcaggattactttcgcaataac
aagtcaacagtagggtaaaactaacctgtctcacgacggtctaaacccag
ctcacgttccctattagtgggtgaacaatccaacgcttggcgaattctgc
ttcgcaatgataggaagagccgacatcgaaggatcaaaaagcaacgtcgc
tatggacgcttggctgccacaagccagttatccctgtggtaacttttctg
acacctcttacctgaaacaatcaggattaaaaggatcgataggccacgct
ttcgcggtctgtactcgtactgaaagtcaagatcaagcaagcttttgccc
ttttgctctacgagaggtttccgtcctctctgagctcgccttaggacacc
tacgttacgatttgatagatgtaccgccccagtcaaactccccgcttgac
actgtcttcgaggagagtcacggtgccataaaatggctccgcttaatgct
tcgaaaaaaggccgtgaagccaattctcttttaaccgaataagtaaagag
tcgatgaaagtggtggtatttcactgtcgtccgaagactcccacctatgc
tacacctctcatgactcttcacaatgtcaaactagagtcaagctcaacag
ggtcttctttccccgctatttttgccaagcccgttcccttggctgtggtt
tcgctagaaagtagttagggacagtaggaatctcgttaatccattcatgc
gcgtcaacaattaaatgacgaggcatttggctaccttaagagagtcatag
ttactcccgccgtttacccgcgcttactcgaattactacgatttaacatt
cagagcactgggcagaaatcagtgacagtcaacgtccgcaaggaccatct
gtcacctctgttttaattagacagtcggattccctgagtccgtaccggtt
ccagtacggttgtttagatgagcgatcaggatactagaaccgaggtccaa
gcacacaccagaaagcgtccgcaagcaagcacaatcactagtccgccatc
aacccgaaagtatcaagcagacagaactgcgccggacaagcatcaaccaa
ctggccaaccgttccaaccactggagccaatccttttcccgaagttacgg
atctagtttgccgacttcccttacctacattattctatcgactagaggct
gttcaccttggagacctaatgcggatatcggtacgattgagtgcaaatta
atagcctcccttggtgttttaagggccgttcaaagagcacgagacaccac
agaaaccgcggtgcttttcggaaacaacgtccccatctctggctgaacca
attccagggagtccgttccttaactagagaagaaaactctagctcggtct

ttgagcgactaaccaagttcgaatgcgttaccgcgcttgtgctccgaaga
acacaatctttgcatctcagttagggaatattaaccctattccctttcga
caagcggggactaaaagcaagcttttcgccaccgatgatacaaggcgttc
gccagtaccttaggatcgactgacccacatccaactactgttcacgtgga
acccttctccacttcagtcttcaaggatcgaacttgaatatttgctacta
ccattacgatctgcactgacggaagctccagccgagcctacgctcatagc
cttcaacgcaaccgccacgaccttcctactcgttacgacctggcgctaga
caacgcacatgtcgcaacggcggagtataggtctctcgcttaagcgccat
ccattttcagggctagttgattcggcaggtgagttgttacacactcctta
gcggataccgacttccatggccaccgtcctgctgtcaatatcaaccaaca
ccttttatggggtctcatgagcgagaagttaggcaccttaactccacgtt
tggttcatcccacagcgccagttctgcttaccaaaaatggcccacttgga
cctcgcattcacgttgacagttcactaaagaaactgcaacttcatatcca
ttgaaagtttgagaataggttgaggacattacgtccccaaggcctctaat
cattagctttaccgaatataactgcctgagatccagctatcctgagggaa
acttcggaaggaaccagctactagatggttcgattagtctttcgccccta
tacccaagtctatcgatcgatttgcacgtcagaaccgatacggacttcca
ccagagtttcctctggcttcatcctgctcaggcatagttcaccatctttc
gggtcgtttgccaactgctcaacctctgcacagtcacaagtgacacgcac
agggccgtggtgcgctgcactccgaagaacacagatcccacgtcggccaa
ttcgagactgacctttactttcatttcgccgcaaggttttaacacccttt
gactcgcagtagacaagcactccgcaatccgtgtttcaagacgggtcgga
aacgtcgtcgactttcacaccgacgtcacacacactagcgtaactaaacg
ctagccgccacgaacccactaccgccagcaagacaccttctcttgcgaga
tgggcaacactgtcgggctagaacgagcagccaacgccgtcggcgtagca
taggaaacgacacccggcaacgatcacaactaagcgaccagtcaccaagc
ttgtctccaagcaacatcaactgtctccggttccactccagcgatttcac
gttctcttgaactctctcttcaaagtcctttgcaactttccctcacggta
cttgttcgctatcgcaatcgagtcgatatttagccttagatgaagtttat
cacccactttaggctgcactttcaagcaacccgactccaaggagcaagcg
aaccaacagtgccgctatccagaacggggctcgcaccctctctggtttat
ggcctcaatcgtaaggacttcggacatacgacactgctggaaacttacac
ctatacgccacatttcgaagcagccaaagactgatcgattcggcgctggg
ctcttcccgtttcactcgccgttactaagggaatccttttagtttcttt
tcctccgctaaatgatatgcttaagttcagcgggtaatcacgactgagtt
caggttgagcgatgatccagctgcaggttcacctacagctaccttgttac
gacttttacccggttcaaaccaatgcgataaaaatggtttccgcaacaac
gaagtcgttaaacctcgaagcgacagtccccactcttctcgaatcagttc
agtcccggatagcgacgggcggtgtgtacaaagggcagggacgtaatcaa

cgtgagctgatgactcacacttactaggcattcctcgtttaagggcaata
attacaataccctatcccggacatggaagaatttcaacggtttaccgata
cctttcggcataggaaaaacccgctgactccaccagtgtagcacgcgtgc
agccccggacatctaagggcatcacagacctgttatcgctcaatctcgtg
cggctaaacaccgcttatccctctaagaagttatacgaacccgaagattc
gccaactatttagcaggctagagtctcgctcgttatcggaataaaccaga
caaatcactccaccaactaagaacggccatgcaccaccaaccaccaaatc
gagaaagagctttcaatctgtcagtcctaatggtgtccggaccgggtgag
ttttcccgtgttgagtcaaattaagccgcaagctccacgccttgtggtgc
ccttccgtcaatttctttaagtttcagctttgcaaccatactacccccgg
aaccgaaagactttcgtttccggatagctcctcggcagggcaaaaaccct
ccgaatcgcgagatggcatcgtttacggtcagaactagggcggtatctaa
tcgccttcgaacctctgactttcgttcttgattaatgaagacattcttgg
caaatgctttcgctgttgggcgtctcactacggtccacgaatttcacctc
tcgcgtaatgatacgaatgcccccggtttgtccctcttaaccattaaatc
agttctagaaccaacaaaaagaaccgaagtcctgtttcattattccatga
tgagctattcaagcaagcgcttgtattgagcactctgatttattcaaggt
aaacctgctggcagttgaagggcgaacccaacctcaaaccagcaaattag
aagtcacgaccacagttgacgcaaattgcgaactgcggcacgtaacctag
atccaactacgagcttttaaccgcagcaataacgagatacactaggaga
cgaagaatcatttgtattcaactcattgaaataactcatccaaaaggatg
agtctttatatttttagtcactatctcatactcaacagtggataagtttc
gcgcctgctgccttccttggacgtggtagccgtttctaaggctccctctc
cggagtcgaacccttattctccgttacccgtaacaaccatggtagtccaa
taaactaccatctagttgaaagggcagacacccttccggatagagtcag
tcgaaactgacagtaaactgctttattcagagtcaacaaacaacgtccga
aaacgtttggtctgttctaataattgcaccccgccttgcgttggggtata
gttgcatgtattagctccagtatttccgcagttatccatatgaggatccc
ggataaggtgatatctgctctaatgagccgtacgcaatttcattgatgaa
tcaaagcatgcatggcttaatcttttacttgagcatatcgcgctgacaga
atcaatcaggtataacaaccctgaaccagacgtaccaactggaggcccag
ttggtgctatgcgttcgaaatttcaccactctaagcgtctgcaattcgtg
agcttacaacatccaggattcccaggccgtctccgatccaagtactaact
ggactcaacgttgcttaacttgccagatcggacgggatggcgtgcattca
acgtgatatggtcgtaagcctgcgttcttcatcgatactcgatgcaaccg
cgcggctgctggcaccagacttgccctctccttgctactccatcgctgaa